

Investigation of In Vivo Cardiac Chambers Composite
Rendering

MUHAMMAD ABDULLAH ADLI BIN AHMAD KAMAL

FACULTY OF ENGINEERING
UNIVERSITY OF MALAYA
KUALA LUMPUR

2021

**INVESTIGATION OF IN VIVO CARDIAC CHAMBERS
COMPOSITE RENDERING**

MUHAMMAD ABDULLAH ADLI BIN AHMAD KAMAL

**DISSERTATION SUBMITTED IN PARTIAL
FULFILMENT OF THE REQUIREMENTS FOR THE
DEGREE OF MASTER OF BIOMEDICAL
ENGINEERING**

**FACULTY OF ENGINEERING
UNIVERSITY OF MALAYA
KUALA LUMPUR**

2021

UNIVERSITY OF MALAYA
ORIGINAL LITERARY WORK DECLARATION

Name of Candidate: Muhammad Abdullah Adli bin Ahmad Kamal
(I.C/Passport No: 901121-13-6261)

Matric No: S2021686

Name of Degree: Master of Biomedical Engineering

Title of Project Paper/Research Report/Dissertation/Thesis ("this Work"):
"Investigation of In Vivo Cardiac Chambers Composite Rendering"

Field of Study: Medical Imaging

I do solemnly and sincerely declare that:

- (1) I am the sole author/writer of this Work;
- (2) This Work is original;
- (3) Any use of any work in which copyright exists was done by way of fair dealing and for permitted purposes and any excerpt or extract from, or reference to or reproduction of any copyright work has been disclosed expressly and sufficiently and the title of the Work and its authorship have been acknowledged in this Work;
- (4) I do not have any actual knowledge nor do I ought reasonably to know that the making of this work constitutes an infringement of any copyright work;
- (5) I hereby assign all and every rights in the copyright to this Work to the University of Malaya ("UM"), who henceforth shall be owner of the copyright in this Work and that any reproduction or use in any form or by any means whatsoever is prohibited without the written consent of UM having been first had and obtained;
- (6) I am fully aware that if in the course of making this Work I have infringed any copyright whether intentionally or otherwise, I may be subject to legal action or any other action as may be determined by UM.

Candidate's Signature

Date: 27/09/2020

Subscribed and solemnly declared before,

Date:

Name:

Designation:

INVESTIGATION OF IN VIVO CARDIAC CHAMBERS COMPOSITE RENDERING

ABSTRACT

Heart disease is the most common cause of death in the world annually. Many fatalities can be avoided if the anomalies in the condition of the heart can be detected earlier for which proper treatment and preventive action can be taken. Detection of this anomalies can be done noninvasively through medical imaging modalities such as by using Computed Tomography (CT) scan. However, accurate interpretation of the heart using 2D images are often hard to do as it is visualized on a flat plane. Therefore, it is important to have a clear representation of the heart using a 3D model which would enable a more accurate interpretation of the heart and its inner chamber to be done for the detection of any anomalies. A 3D model reconstructed through the VTK program software using layers of 2D CT scan images are therefore proposed for this purpose. In this study, 399 layers of 2D CT scan image was used for the 3D model reconstruction. As a comparison, another 3D model was also reconstructed with the same 2D CT scan images using another software, 3D slicer. Although both software is able to reconstruct a good model of the heart, VTK appears to be the superior option for investigating the inner chambers of the heart. Both software also allows the measurement of the length between two points which enables the length of object under investigation to be estimated. In conclusion, VTK is able to reconstruct a good 3-dimensional representation of the heart which helps medical practitioners to better detect anomalies in their patients.

Keywords: Cardiac Chamber, Computed Tomography (CT) Scan, 3D Reconstruction model, visualization toolkit (VTK), Volume Rendering

PENYELIDIKAN PERSEMBAHAN KOMPOSIT DALAM VIVO RUANG JANTUNG

ABSTRAK

Penyakit jantung adalah penyebab kematian yang paling utama di dunia setiap tahun. Banyak kematian dapat dielakkan jika anomali dalam keadaan jantung dapat dikesan lebih awal untuk rawatan dan tindakan pencegahan yang tepat. Pengesanan anomali ini dapat dilakukan secara tidak invasif melalui kaedah pengimejan perubatan seperti dengan menggunakan imbasan Computed Tomography (CT). Walau bagaimanapun, penafsiran jantung yang tepat menggunakan gambar 2D sering sukar dilakukan kerana ia dilihat pada satah rata. Oleh itu, adalah penting untuk mempunyai gambaran jantung yang jelas menggunakan model 3D yang akan membolehkan penafsiran jantung dan ruang dalamnya dengan lebih tepat untuk mengesan sebarang anomali. Oleh itu, model 3D yang dibina semula melalui perisian program VTK menggunakan lapisan gambar imbasan CT 2D dicadangkan untuk tujuan ini. Dalam kajian ini, 399 lapisan gambar imbasan CT 2D digunakan untuk pembinaan semula model 3D. Sebagai perbandingan, model 3D lain juga disusun semula dengan gambar imbasan CT 2D yang sama menggunakan perisian lain, 3D Slicer. Walaupun kedua-dua perisian ini dapat menyusun semula model jantung yang baik, VTK dilihat sebagai pilihan yang lebih baik untuk menyelidiki ruang dalaman jantung. Kedua-dua perisian ini juga mempunyai fungsi pengukuran panjang antara dua titik yang memungkinkan panjang objek yang disiasat dapat dianggar. Kesimpulannya, VTK dapat membina semula gambaran jantung 3 dimensi yang baik yang membantu pengamal perubatan untuk mengesan anomali pada pesakit mereka dengan lebih baik.

Kata kunci: Ruang Jantung, Imbasan Tomografi (CT), Model Rekonstruksi 3D, VTK, Persembahan Isipadu

ACKNOWLEDGEMENTS

The completion of this study is made possible through the assistance of many individuals in particular:

My supervisor, Mr Lai Khin Wee who had taught me regarding medical imaging, medical imaging application software and guides me through the completion of the study.

My fellow classmates in medical imaging class who had been much of help in learning the use of the medical application software together.

My parents, Ahmad Kamal and Adilah Hanim, from whom I owe my existence, support and best wishes.

Everyone who had been of help indirectly through their kindness and support,

I sincerely express my gratitude.

Thank you.

TABLE OF CONTENTS

Abstract	iii
Acknowledgements	v
Table of Contents	vi
List of Figures	viii
List of Symbols and Abbreviations.....	xi
CHAPTER 1: INTRODUCTION.....	1
1.1. Problem Statement	3
1.2. Aims and Objectives	4
CHAPTER 2: LITERATURE REVIEW.....	5
2.1. Two-dimensional (2D) Computed Tomography (CT) Imaging	5
2.2. Computed Tomography (CT) Imaging of the Heart	7
2.3. Three Dimensional (3D) CT Scanning Reconstruction Process	8
2.3.1. Interpolation.....	9
2.3.2. Volume Representation on a Flat Screen.....	10
2.3.3. Assigning a value to the screen pixel	11
2.3.3.1. Sum	11
2.3.3.2. Maximum intensity projection (MIP)	12
2.3.3.3. Shaded surface display (SSD).....	13
2.3.3.4. Volume rendering and percentage classification	13
2.3.4. Multiplanar reformatting (MPR)	14
2.3.5. Depth perception enhancement.....	15
2.3.6. Segmentation	16
2.4. DICOM Images.....	17
2.5. Visualisation Tool Kit (VTK)	18
2.5.1. Image Processing in VTK.....	19
2.5.2. Volume Rendering Using VTK.....	19
2.5.3. Medical Applications of VTK	20
2.6. 3D Slicer	22
2.7. Analysis of the Cardiac Chamber	23
2.7.1. Two-Chamber Views.....	24
2.7.2. Three-Chamber View	25
2.7.3. Four-Chamber View	26
CHAPTER 3: METHODOLOGY.....	28
3.1. 2D CT Image Acquisitions.....	29

3.2. Volume Rendering Process	29
3.3. Coding.....	32
3.3.1. Volume Rendering of the 2D CT-Scan Cardiac Images	32
3.3.2. Surface Rendering of the Heart Chamber.....	38
CHAPTER 4: RESULTS.....	41
4.1. 3D Reconstruction of Cardiac Chamber Image	41
4.2. Comparison with Cardiac Chamber Image Reconstruction using 3D slicer.....	45
4.3. Measurement of the heart using VTK and 3D slicer	49
CHAPTER 5: DISCUSSIONS	53
5.1. 3D Reconstruction of Cardiac Chamber Image	53
5.1.1. Visualization of the Right Atrium and the Right Ventricle.....	54
5.1.3. Image Noise Reduction.....	56
5.1.4. Comparison with Surface Rendering Images	57
5.2. Comparison with image produced using 3D slicer	59
5.3. Measurement of the heart using VTK and 3D slicer	61
CHAPTER 6: CONCLUSION.....	62
References	64

LIST OF FIGURES

Figure 1. 1: Volumetric biomedical imaging data acquisition with a CT scanner.....	6
Figure 2. 1: Representation of images in three-dimensional space to produce a cube of data	9
Figure 2. 2: Comparison between image obtained using (a) a 256 x 256 image matrix and (b) 512 x 512 image matrix.	10
Figure 2. 3: Ray casting. In this procedure, virtual lines are projected from the flat panel to the volume.....	11
Figure 2. 4: The sum of all voxels in the volume produces the standard roentgenogram.	11
Figure 2. 5: MIP image is created by merging several contiguous slices and projecting the highest attenuation	12
Figure 2. 6: Bones and tissues distinguished by their density and colour scale in volume rendering	14
Figure 2. 7: In multiplanar reformation, interpolation of known volume allows the points of the plane crossing the volume to be obtained	15
Figure 2. 8: Application of segmentation tools for organ's exact volume measurement	16
Figure 2. 9: Digital Imaging and Communication in Medicine (DICOM)	17
Figure 2. 10: DICOM layers	17
Figure 2. 11: Conceptual overview of the VTK pipeline.....	19
Figure 2. 12: Volume Rendering Pipeline Overview in VTK	20
Figure 2. 13: 2-Chamber view. LA = left atrium, LV = left ventricle	24
Figure 2. 14: Medical conditions depicted using the two-chamber view. (A) Left ventricular chamber dilation caused by dilated cardiomyopathy. (B) Isolated left ventricular hypoplasia.	24
Figure 2. 15: 3-Chamber view. LA = Left Atrium, Ao = aorta, LV = Left Ventricle	25
Figure 2. 16: Pathologies depicted through three-chamber view. (A) Low density vegetation on the right and left coronary cups in patient with infective endocarditis. (B) Paravalvular pseudoaneurysm (arrowheads) and small vegetation (arrow).	25

Figure 2.17: 4-chamber view. LA = left atrium, LV = left ventricle, RA = right atrium, RV = right ventricle.	26
Figure 2. 18: Medical conditions depicted through the four-chamber view. (A) Dilation of the right ventricle (RV) caused by atrial septal defect (asterisks). 1. Basal RV diameter, 2. Mid-RV diameter, 3. RV length from base to apex. (B) Membranous ventricular septal aneurysm (arrow). (C) Patent foramen ovale with a left-to right shunt (arrow). (D) Dilation of RV chamber caused by arrhythmogenic RV dysplasia.	27
Figure 3. 1: VTK Visualization Pipeline.....	29
Figure 4. 1: General structure of the heart	41
Figure 4. 2: Isometric view of the overall 3D model.	41
Figure 4. 3: Axial view of the heart. (DA-Descending Aorta, AA-Ascending Aorta, MPA-Main Pulmonary Artery, LPA-Left Pulmonary Artery and RPA-Right Pulmonary Artery).....	42
Figure 4. 4: Sagittal view of the heart. (MPA-Main Pulmonary Artery, RVOT-Right Ventricular Outflow Tract, LA-Left Atrium and MV-Mitral Valve).	42
Figure 4. 5: Coronal view of the heart. (MPA-Main Pulmonary Artery, AA-Ascending Aorta, AV-Aortic Valve, and LV-Left Ventricle).	43
Figure 4. 6: Two chamber view of the heart. (LA-Left Atrium, MV-Mitral Valve and LV-Left Ventricle).....	43
Figure 4. 7: Three chamber view of the heart. (LA-Left Atrium, MV-Mitral Valve, LV-Left Ventricle, AV-Aortic Valve and AA-Ascending Aorta).....	44
Figure 4. 8: Four chamber view of the heart. (LA-Left Atrium, LV-Left Ventricle, RA-Right Atrium and RV-Right Ventricle).....	44
Figure 4. 9: Views of different planes generated on a single window using 3D Slicer ..	45
Figure 4. 10: Pre-set Options for Display of 3D Model using 3D slicer	46
Figure 4. 11: Volume Properties Adjustment using 3D slicer	46
Figure 4. 12: Isometric view of the overall 3D model using 3D slicer	47
Figure 4. 13: Axial view of the heart using 3D slicer	47
Figure 4. 14: Sagittal view of the heart using 3D slicer.....	48
Figure 4. 15: Coronal view of the heart using 3D slicer	48

Figure 4. 16: Four Chamber view of the heart using 3D slicer.....	49
Figure 4. 17: Width of the heart measurement using VTK.....	50
Figure 4. 18: Width of the heart measurement using 3D slicer	50
Figure 4. 19: Height of the heart measurement using VTK.....	51
Figure 4. 20: Height of the heart measurement using 3D slicer.....	51
Figure 4. 21: Length of the heart measurement using VTK	52
Figure 4. 22: Length of the heart measurement using 3D slicer	52
Figure 5. 1: Source image.	54
Figure 5. 2: (a) Four Chamber View of the heart where the right atrium and right ventricle are made visible after opacity and colour setting adjustment. The yellow box shows the area where the structure of the septum is compromised. (b) Four Chamber View of the heart in the original setting where the right atrium and right ventricle is barely visible	55
Figure 5. 3: Sagittal View of the heart. (a) The yellow box indicates the area where the structure of the septum is compromised after some adjustment in opacity and colour setting to make the right atrium and ventricle more visible. (b) Sagittal View of the heart in the original setting where the right ventricle is barely visible	55
Figure 5. 4: Sagittal view of the heart (a) before and (b) after image noise reduction ...	56
Figure 5. 5: Axial view of the heart (a) before and (b) image noise reduction.....	56
Figure 5. 6: Isometric view of the overall model using the (a) surface rendering technique and (b) volume rendering technique	57
Figure 5. 7: Axial view of the heart using (a) surface rendering method and (b) volume rendering method	57
Figure 5. 8: Sagittal view of the heart generated using (a) surface rendering method and (b) volume rendering method.....	58
Figure 5. 9: (a) Axial, (b) sagittal and (c) coronal view of the heart generated using data set 2 through VTK programme.	60
Figure 5. 10: (a) Axial, (b) sagittal and (c) coronal view of the heart generated using data set 2 through 3D slicer programme.	60

LIST OF SYMBOLS AND ABBREVIATIONS

2D	:	Two-dimensional
3D	:	Three-dimensional
CAT		Computerized axial tomography
CT	:	Computed Tomography
DICOM		Digital Imaging and Communications in Medicine
HUs		Hounsfield units
MIP		Maximum Intensity Projection
MinIP		Minimum Intensity Projection
MPR		Multiplanar reformatting
MRI	:	Magnetic Resonance Imaging
PACS		Picture archiving and communication systems
RGB	:	Red Green Blue
ROI	:	Region of Interest
SSD		Shaded surface display
VTK	:	Visualization Toolkit

CHAPTER 1: INTRODUCTION

Medical imaging has a long history since the discovery of X-rays by Wilhelm Conrad Roentgen in 1895, for which he won the first Nobel prize (Tubiana, 1996). Many diseases and abnormalities can be detected through medical imaging. Medical imaging is a technique used to capture the visual orientation of a specimen's interior and also visualize the functioning of its organs or tissues. The technique is useful in various applications such as to diagnose a patient's condition, analysing archaeological and fossils specimens and so on (Ghoshal et al., 2020).

Heart disease is the most common cause of fatalities worldwide. According to the World Health organization (WHO), ischaemic heart disease accounts for 16% of the world's cause of death in 2019. In fact, since 2000, the largest increase in the cause of death is seen in this disease, soaring by about 2 million cases to 8.9 million deaths in 2019 (World Health Organization, 2020). Many of such fatalities can be prevented if the onset of the heart diseases were detected much earlier so that proper treatment and preventive action can be taken to prevent the condition from worsening. Medical imaging provides a practical non-invasive solution to solve this problem (Chaosuwannakit, 2018). However, the accuracy of the detection and interpretation such images depend on the quality of the image used itself. Therefore, a good medical imaging modalities are required so that the anomalies inside the heart can be detected easily and with great accuracy.

Computed Tomography (CT) scan utilize X-rays to visualize specific parts the body. A safe amount of radiation is used to generate detailed images that helps doctors to detect problems in that particular area of the body. Prior to the scan, a specialized dye (usually iodine) is injected into the bloodstream which will then be viewed using a special camera in the hospital (Pan et al., 2016). If used for viewing arteries that allow the supply of blood to the heart, heart CT scan may also be called coronary CT angiogram. If the

visualization purpose is to identify calcium build up in the heart, the CT scan may also be termed as coronary calcium scan (Krans, 2017).

CT scan of the heart are generally performed to detect problem or medical condition related to the heart. They may include congenital heart disease (birth defects in the heart), build-up of lipid-based plaque which may blocks the coronary arteries, injury, defects or deformity at hearts four primary valves, blood clotting within the chambers of the heart or even tumour formation inside or on the surface of the heart. The benefit of heart CT scan is that it allows medical personnel to examine the heart structure and the surrounding blood vessels without the need to perform an intrusive cardiac operation or incision. CT scan images may also be used for pre-surgery planning to identify the spatial relationship between the region of interest such as the pathological lesions and the surrounding structures as well as planning for radiotherapy (Wang et al., 2015).

However, just visualizing 2D images of CT scan is not enough to identify problem inside the body let alone a complex structure such as the internal chambers of the heart. Flat 2D images are often hard to interpret as tissues and organs look much differently in two-dimension when compared to the way they actually look in real life which is in 3-dimension. The internal structure of tissues and tissue lesion are especially hard to interpret correctly and this can lead to misdiagnose of medical conditions. Various anatomical structures may overlap, creating a camouflaging effect that complicates the interpretation of the medical images (Krupinski, 2010). Furthermore, the process of browsing through slices by slices of 2D images in different cross-sectional views are very tedious and inefficient. Therefore, visualization in 3D is often needed to get a full picture of the patient's organ and to easily identify any anomalies. This is especially so in a complex organ such as the heart.

3D reconstruction techniques are generally divided into two types, surface rendering and volume rendering. In surface rendering, the 3D objects' surface is reconstructed and

preserved and it has the advantage of having relatively small amount of contour data resulting in accelerated rendering speeds (Pei, 2019). In volume rendering, the internal structure of 3D object is reconstructed from layers of 2D images for volumetric view visualization. Therefore, when the 3D image model is sliced into 2D, the internal structure of the object can also be viewed.

As the image processing technology advances, the role of 3D medical image as a tool for medical diagnosis has becomes more prominent as it provides swath of detailed information that can be utilized by clinicians. This includes its application in the detection of diseases and anomalies inside body including the heart.

1.1. Problem Statement

2D Medical images produced through computerized tomography (CT) scan are often hard to interpret on a flat plane which can lead to wrongful diagnosis. This could result in the wrong treatment being prescribed or certain anomalies being missed out from detection. Such misdiagnosis or misdetection could prove to be fatal. If the anomalies are detected earlier, proper treatment could be administered to prevent the disease or medical condition from deteriorating. This is especially so in a complex and crucial organ such as the heart. Furthermore, the process of browsing through layers by layers of 2D images in different cross-sectional views are very tedious and inefficient. A way of visualizing 2D CT images in 3D are therefore needed to make a more accurate and easier interpretation of medical images of the heart.

1.2. Aims and Objectives

The aim of this study is to develop a 3D model for a better visualization of the cardiac chamber based on layers of 2D CT scan images using the VTK program for easier and more accurate interpretation of the heart images.

Objectives:

- a. To visualize the cardiac chamber through the application of 3D reconstruction algorithm using Visualization Toolkit (VTK)
- b. To compare the 3D reconstruction model formed using Visualization Toolkit (VTK) and 3D Slicer.

CHAPTER 2: LITERATURE REVIEW

This section elaborates about the Computed Tomography (CT) imaging system, the reconstruction of its 2D image slices into a 3D model, its application in cardiac imaging with different section views, as well as some introduction regarding the VTK and 3D Slicer software.

2.1. Two-dimensional (2D) Computed Tomography (CT) Imaging

Computed tomography (CT), otherwise known as computerized axial tomography (CAT) imaging utilize specialized equipment emitting X ray to create cross sectional images of the body. In conventional CT scanner, the X ray source and detectors with a circular metal frame rotate around the patient that are laid down in a horizontal position on a movable table which would then be passed slowly through the centre of the CT scanning machine. The procedure itself will not cause any pain, but in some cases, contrast materials are needed to distinguish between the different tissues in the body and to allow area of concern to be made more prominent for better visualization (Karatas & Toy, 2014).

CT scan is an anatomical imaging modality which captures the image of the organs, soft tissues and dense skeleton. It is used for the diagnosis of many disorders including fractures, tumours, haemorrhage, disease inflammation, bowel obstruction as well as kidney stones. It generates high resolution volumetric images that are especially suitable for the inspection of dense structures including bone or lung tissues. The attenuation of X rays for different anatomical structures are predictable and this range of intensity is represented by Hounsfield units (HUs). Different structures such as the brain, bone and soft tissues can be categorized using HUs and in conjunction with contrast agents may also help to identify the structures (Kim et al., 2020). As an example, contrast agents in

combination with rapid CT scanning in angiography enables the vasculature images to be visualized.

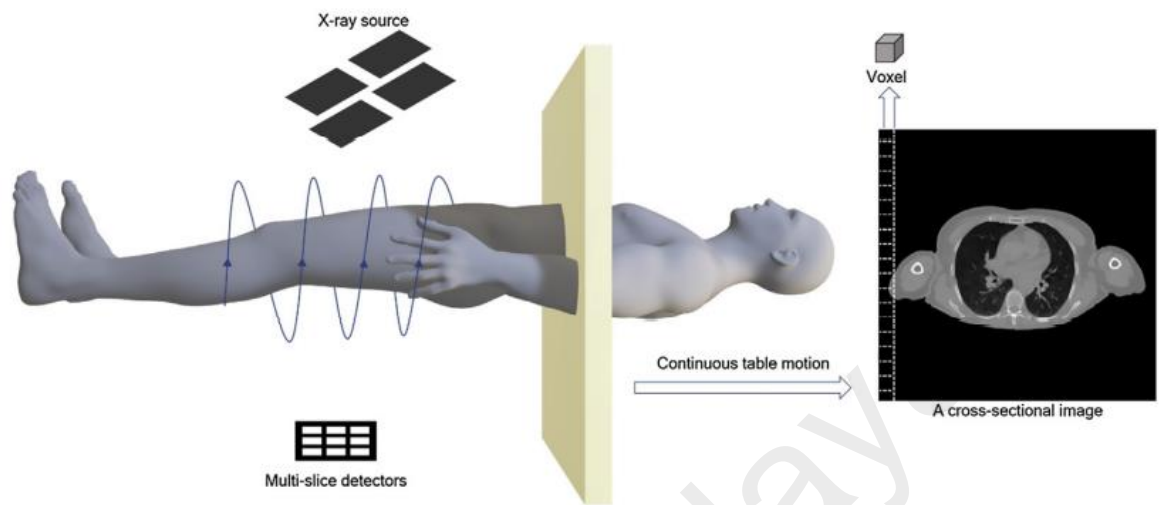


Figure 1. 1: Data acquisition of volumetric biomedical imaging using a CT scanner

Basically, the CT scanner functions with the following steps: After the patient had lie down on the motorized table, the table would be moved together with patient along a circular opening at the centre the CT scanning machine. When the patient indicates their readiness, the operator will initiate the CT imaging system which starts with a complete rotation of the source and detector lasting for around 1 second. The CT scanning system will create a narrow, fan shaped beam of X-rays that scans a section of the patient's body. A still image of that particular section of the body will be captured by the detector located opposite of the x-ray source. The data acquired would then be transmitted to a computer each time the scanner and detectors turned. Multiple cross-sectional images of the body parts can be captured and reconstructed. The desired image would be formed once the multiple images of the patient, scanned successively in the axial plane section are combined. An advanced CT scan can scan 64 or 128 sections at one time. This system would save time as it can be performed quicker and required low dosage of X rays (Aboudara et al., 2003). However, it is quite expensive as it need a lot of sensors. Organs

are not superposed on each other using this technique, as the tissues are sectioned (Karatas & Toy, 2014).

Despite its high price and high radiation dose, the benefit of CT scan outweighs the risk in certain conditions. It has many applications in detecting tumours, haemorrhage, infarction, bone trauma, calcifications, inflammations as well as cancers. It is can also be used to perform coronary angiography to assess the coronary arteries of the heart.

2.2. Computed Tomography (CT) Imaging of the Heart

CT images can provide a very high-quality images for cardiovascular imaging of the proximal epicardial vessels, with quality that equals to or even surpassing the ones obtained through the invasive conventional angiography. They can also be used to diagnose pulmonary embolism, aneurism, aortic and coronary arteries dissections as well as arteriovenous malformations (Ou, et al., 2007).

The leading modality for investigating the intracardiac structures in children are cardiac ultrasound. However, it is often inadequate to study certain structures of the heart such as the aorta, coronary arteries, pulmonary artery branches and systemic and pulmonary venous structures. These structures are better visualize using CT as it has better diagnostic capability due to its high precision 3D imaging (Goo et al., 2005). Three-dimensional imaging is especially useful to detect and investigate complex form of congenital disease, as a preparation for complex interventional procedures that requires cardiac catheterization as well as for the assessment of surgical reconstruction, post operation. However, it is often quite difficult to obtain a good quality image for children under the age of 5 years old due to their tendencies to be anxious and agitated which creates respiratory and cardiac movement artifacts. Therefore, their images are often

taken as quickly as possible when they are lightly sedated or in the state of calmness (Ou, et al., 2007).

The diagnosis of congenital abnormalities for adults often made use of CT coronary angiography as they provide accurate and precise description of the there-dimensional anatomy of the coronary arteries. CT coronary angiography is often useful to detect complications post coronary operations that fix the congenital cardiac abnormalities (Schroeder, et al., 2008).

Other non-radiation-based applications such as the magnetic resonance imaging (MRI) are theoretically more desirable particularly in children, if the screening examinations have to be taken repeatedly. That being said, due to their relatively poor temporal resolution (especially for coronary arteries assessment), as well as their complex protocol and time-consuming image acquisition (thus necessitating the use of general anaesthesia in young children), MRI usage in heart imaging has been limited (Taylor et al., 2005).

2.3. Three Dimensional (3D) CT Scanning Reconstruction Process

CT scanning creates a series of two-dimensional pictures which can be layered on top of one another to create a three-dimensional image. These layers of two-dimensional image are separated by gaps that needs to be filled in to create a continuous volume of data (Figure 2.1). This can be done by a process called interpolation. Two-dimensional images are formed by a combinations of picture elements called pixels. The equivalent of pixels for three-dimensional images are called volume elements (voxels). In this case, pixels and voxels may be referred to as points for the sake of simplicity.

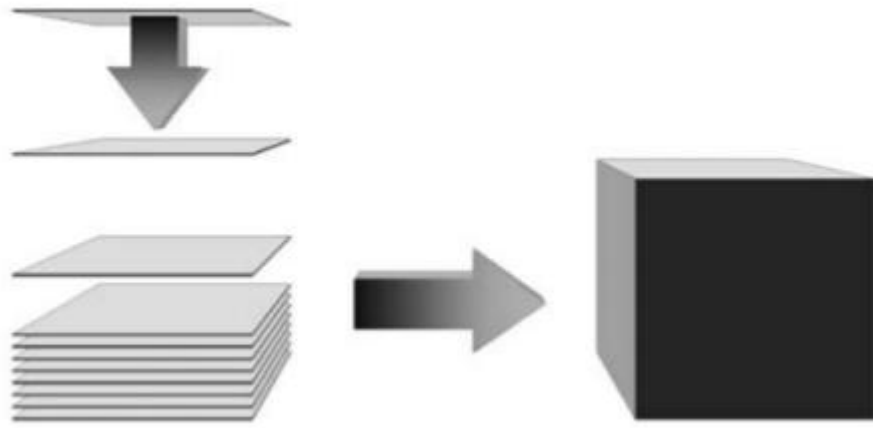


Figure 2. 1: Representation of images in three-dimensional space to produce a cube of data

2.3.1. Interpolation

Missing values from known surrounding points can be estimated using interpolation (Lichtenbelt et al., 1998). This has been the practice to reconstruct three dimensional images in CT scanning. It should be assumed that each location has its own value. Using the nearest neighbour interpolation, the missing values are obtained from the values of the nearest point. Using linear interpolation, the missing values are acquired through the linear relationship between two known adjacent points. As this operation is not radial in nature, it may result in cross-shaped artefacts. Cubic convolution interpolation may solve this issue as the missing values are allocated values from four or more points. This radially operated function is expensive computationally wise. The major requirement for this operation is that the distances between the points are quite small enough that the missing values can be assumed between the surrounding points (Luccichenti, et al. 2005). Should this not be the case, incorrect values may be assigned to the missing values points. It needs to be pointed out that interpolation does not result in the creation of new information. What it does is simply increasing the number of points from which this information is represented by assigning values to points where values are missing (Figure 2.2).

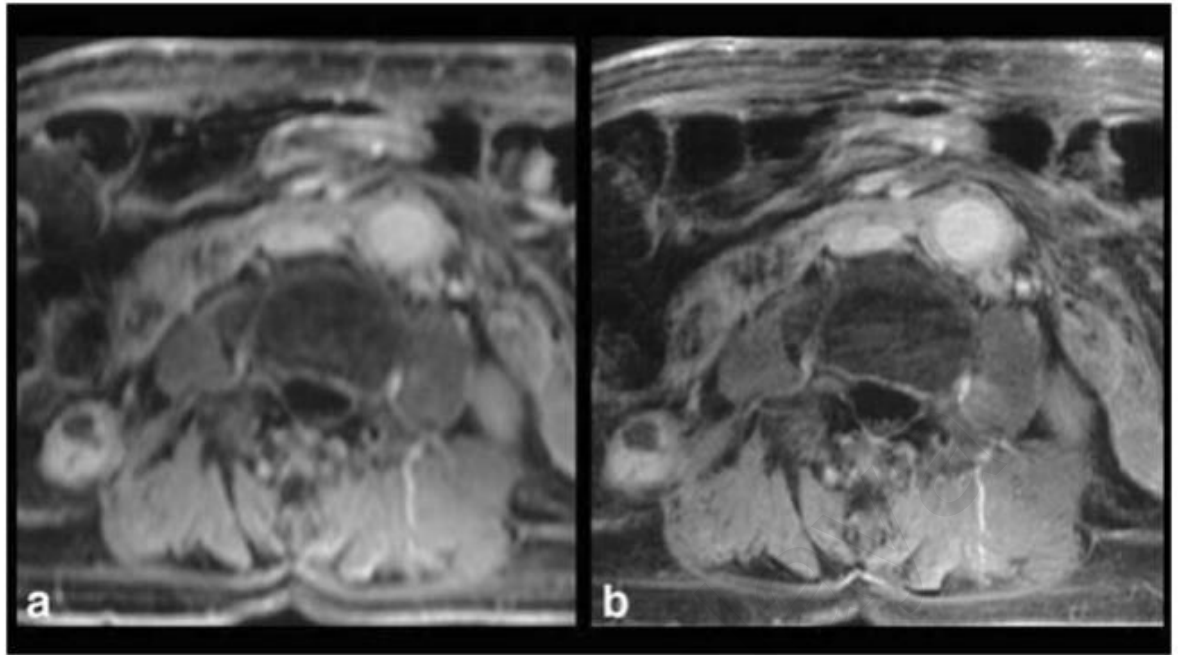


Figure 2. 2: Comparison between image obtained using (a) a 256 x 256 image matrix and (b) 512 x 512 image matrix.

2.3.2. Volume Representation on a Flat Screen

Volume representation in a two-dimensional picture can be attained by projecting voxels which form the volume on a surface. As the screen for which this volume is projected are flat, the voxels forming the volume may not necessarily correspond to the pixels of the screen. In order to avoid fractional values, ray casting is performed (Calhoun et al., 1999). In this operation, rays are projected from the screen's pixel to the volume's voxels (Figure 2.3). However, the projected rays may not necessarily correspond to the volume's voxels. In such case, interpolation is used to acquire the value of the points forming the rays. Depth perception can be augmented by ray building from a hypothetical observer point of view. The visualisation of the structures is affected by the geometry of the projection. Optimum projection is obtained if it displays wide surface with minimal distortion.

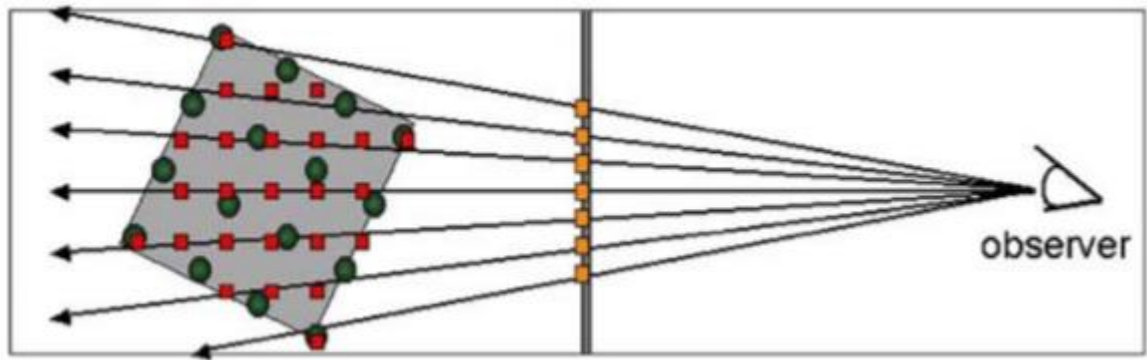


Figure 2. 3: Ray casting. In this procedure, virtual lines are projected from the flat panel to the volume.

2.3.3. Assigning a value to the screen pixel

2.3.3.1. Sum

The value of the pixel where the ray is cast from is equal to the sum of the values of the points along the ray. The image produced resembles what is seen in a standard roentgenogram (Figure 2.4).

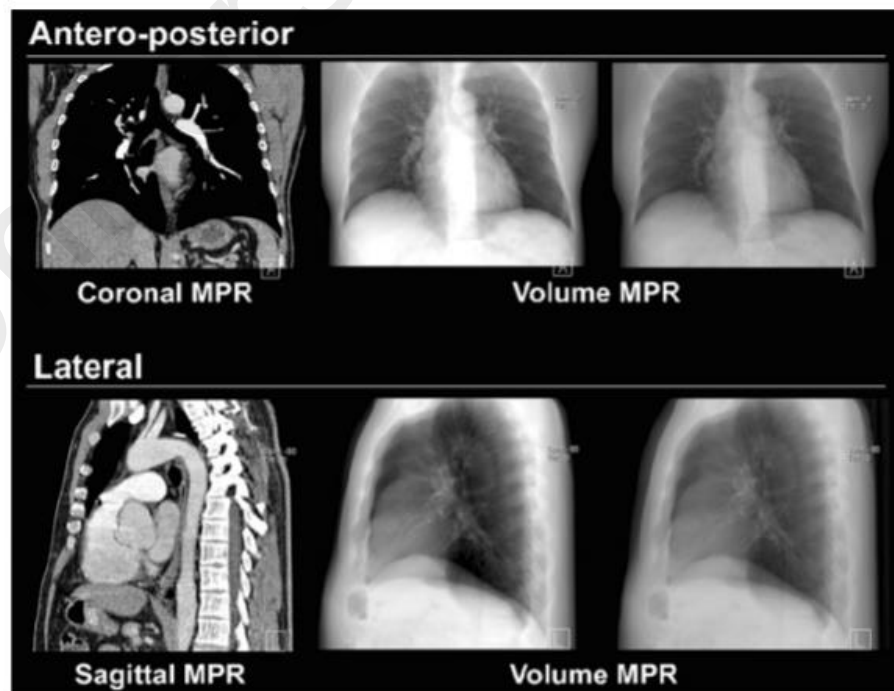


Figure 2. 4: The sum of all voxels in the volume produces the standard roentgenogram.

2.3.3.2. Maximum intensity projection (MIP)

Should the value of the pixel be equivalent to that of the interpolated voxel with the highest value across the ray, Maximum Intensity Projection (MIP) image would be resulted. In contrast, the pixel value set to the lowest value along the ray would result in the Minimum Intensity Projection (MinIP). The disadvantage of MIP is that it does not represent voxels with values that are not the highest along the ray. As a result, structures with hypo-intensity could be masked with hyper intense structure as only materials with the highest intensity along the projected ray is represented. Additionally, in the absence of depth cues, superimposed structures may also be formed when two separate hyper intense structures are present along the rays (Sato et al., 1998). In order to avoid this problem, the volume may be rotated to acquire different projection views and be further analysed. The overlapping structures may be excluded by trimming the volume and this would also reduce the computational requirement. Unfortunately, the measurement in MIP image is not reliable due to its projective nature.

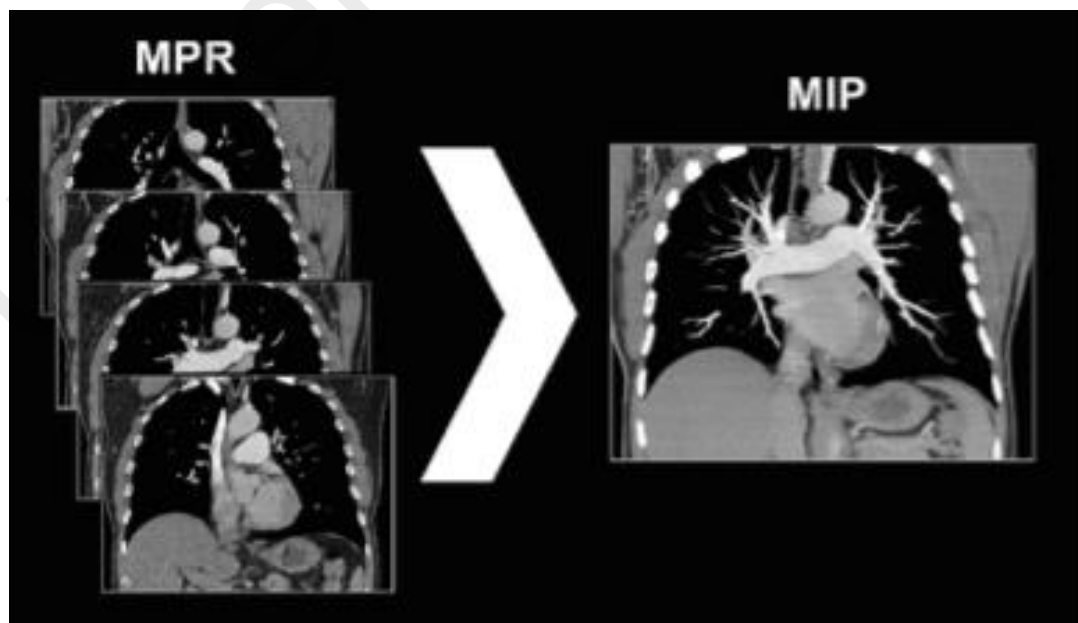


Figure 2. 5: MIP image is created by merging several contiguous slices and projecting the highest attenuation

2.3.3.3. Shaded surface display (SSD)

In shaded surface display which represents the structure's surface, the value of the pixels in the final picture correlates to the point's value that is closest to the screen and above a certain threshold which decide how close the resultant image represents the actual anatomy. This type of image however does not give information regarding the density of the tissues within. This would present a lot of densitometric associated problems. For example, should the threshold selected are incorrect, a stool in colonography examination may misleadingly appears to be part of the mucosa thus resembling a tumour formation. Another example, calcified formations on the vascular structures and the contrast agent may appears to be the same on the image display (Semba et al., 1994). Depth perception can be enhanced by implementing a shading scale with depth encoding that would make closer voxel appears brighter and vice versa.

2.3.3.4. Volume rendering and percentage classification

The contribution of each point along the ray towards the formation of pixel value of a picture is defined using the classification operation which may range from 0 to 100% opacity (Luccichenti, et al. 2005). The voxel value is correlated with its opacity using the opacity function curve. Thus, the opacities contribution of the points along the ray results in the pixel value that appears on the screen. Only voxels with values that are situated within selected intervals would be represented while the ones outside the intervals would appears transparent. In computed tomography, voxel values are reflected from the attenuation of X-rays projected in Hounsfield Units (HU). The visibility of the structures is determined by the shape of the curve corresponding to their attenuation (Fishman, et al., 1991). The pixel value is representable through the use of grey or colour scale that can intensify the depth perception as well as the density-based information. In contrast

with SSD where the pixel values depend on the virtual distance of the volume from the screen, the pixel values in volume rendering (VR) depends on the densitometric information that it contains. Thus, volume rendering produce both spatial as well as the densitometric information. Similar to MIP and SSD however, the measurement produced in the VR images are not reliable as the setting for opacity and rendering have strong effects on the visibility and the dimensions of the structures.

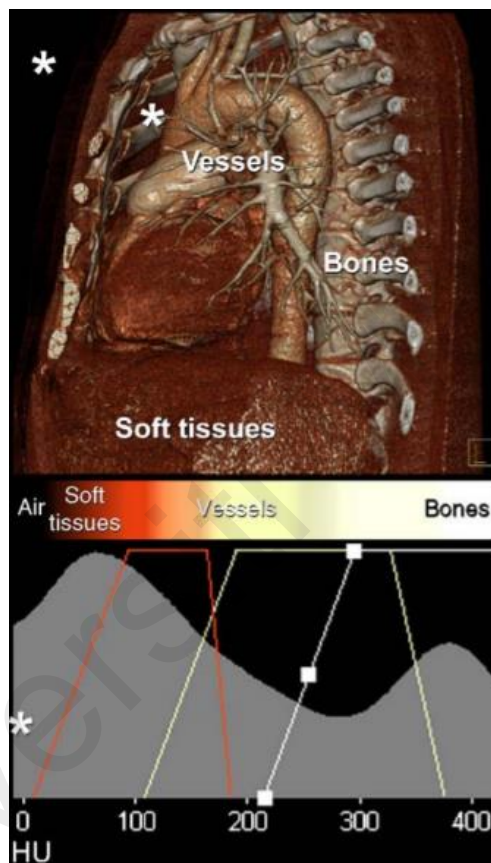


Figure 2. 6: Bones and tissues distinguished by their density and colour scale in volume rendering

2.3.4. Multiplanar reformatting (MPR)

Multiplanar reformatting images are generated from native image slices layered in different plane. Interpolation from the closest voxels is used to assign values to the pixels that forms the reformatted plane. “Thick slab” is formed when distant voxels also contribute to the final picture (Dalrymple et al., 2005). In the same way, pictures of a

curved plane situated along a vessel can be acquired. The utility of MPR is in its utilization for assessing the structure's spatial relationship oriented in the scan plane. Additionally, measurement errors of a structure that is oriented obliquely with respect to the scan plane can be avoided.

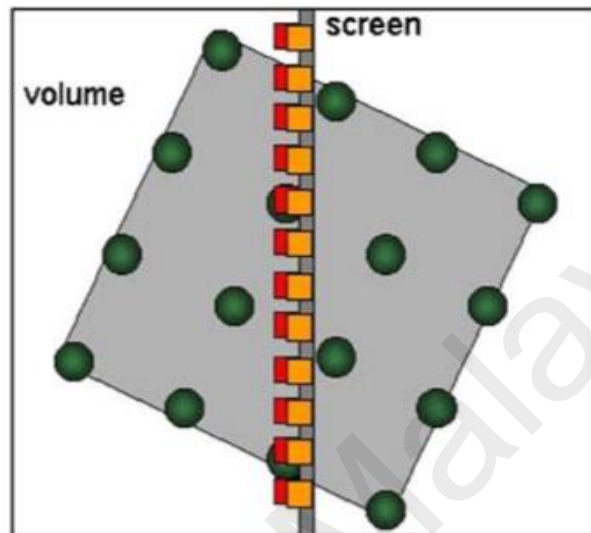


Figure 2. 7: In multiplanar reformation, interpolation of known volume allows the points of the plane crossing the volume to be obtained

2.3.5. Depth perception enhancement

In volume rendering, estimation of gradient of variation of the voxel's values within a volume is the principle by which the surfaces are identified by. This had been especially helpful when used for illumination and shading operation (Udupa, 1999). In other words, modification of the surface colour according to the angle of light incidence that originates from a virtual source is the basis of what illumination operation is all about while light intensity in the scene is the basis for which colours are modified in shading operations. Additionally, light reflection is affected by the texture of the surface, in which case a smooth surface tends to reflect light better than an irregular one.

2.3.6. Segmentation

The voxels forming an object within the volume are labelled through segmentation. This process can be performed manually, automatically or even semi automatically through a software whereby morphology, homogeneity, density, inherent structure and location within the volume is the basis from which an object can be identified by (Masutani et al., 2001). The object needs to have at least one feature that enable it to be identified, failing which, an accurate segmentation will not be possible. The presence of various tissues and structures with similar densities around or connected to an object is quite a challenge for the segmentation process. Manual setting of a threshold using morphological operations or advanced algorithm allows the object margins to be defined (Paik et al., 1998). In this way, the margins of non-tissue structures can be defined using hypodense fatty layers. Using the vessel lumen's high differential density in contrast to the surrounding structures, allows the vascular structures to be segmented manually or even automatically. This had also been the principle by which virtual CT colonoscopy is implemented by. Accurate evaluation and analysis of volume, surface or the histogram of the segmented object is also made possible by segmentation (Frerick et al., 2004). Additionally, segmentation is a fundamental operation for hollow viscera unwrapping and automated lesion detection which is very important during screening programs (Summers et al., 2000).

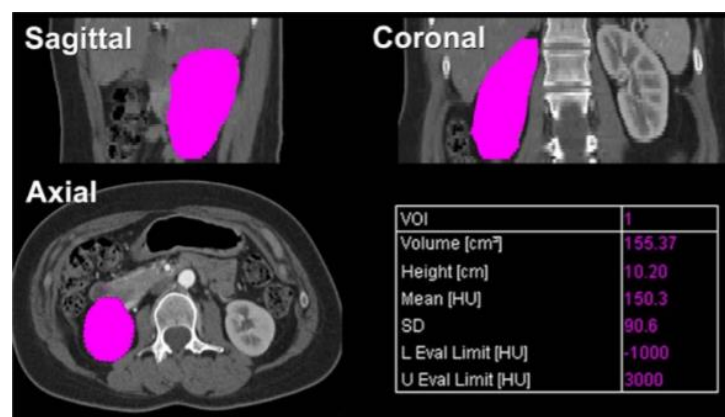


Figure 2. 8: Application of segmentation tools for organ's exact volume measurement

2.4. DICOM Images

The CT images used in this study are DICOM images. DICOM or Digital Imaging and Communications in Medicine is the standard for communication and management of data related to medical imaging information. It is frequently utilized for data processing as well as for printing, storing and transmission of medical images which allows the integration of medical devices such as printers, scanners, servers, network hardware, workstations and picture archiving and communication systems (PACS) from various different manufacturers. It is most commonly used in hospitals as well as other medical facilities. The DICOM standards utilize a communication protocol to coordinate network communication and exchange of patient images and data using TCP/IP for inter-system communication. DICOM utilize layers of images that are integrated through a special system that clearly shows the resultant combined rays clearly (**Figure 2.10**)(Mamdouh et al., 2020).

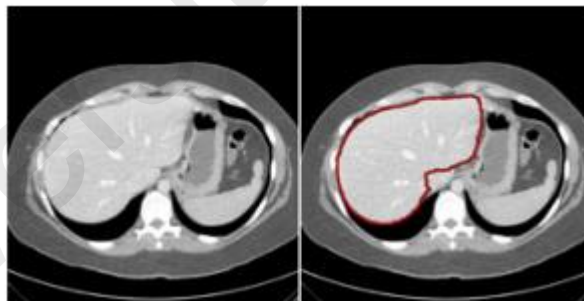


Figure 2. 9: Digital Imaging and Communication in Medicine (DICOM)

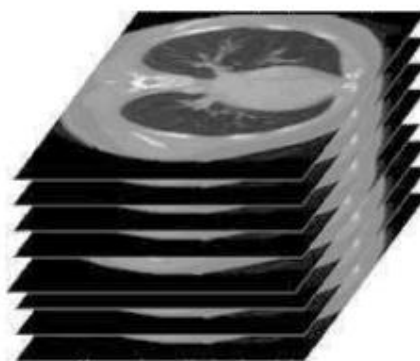


Figure 2. 10: DICOM layers

2.5. Visualisation Tool Kit (VTK)

The Visualization Toolkit (VTK) is a widely used C++ class library for visualization. It supports various visualization algorithms including scalar, tensor, vector, texture and volumetric methods as well as advanced modelling techniques including implicit modelling, mesh smoothing, contouring, cutting, polygon reduction and Delaunay triangulation. VTK is an important resource for a cost effective, rapidly developed medical imaging tools. Its most widely used application is in two and three-dimensional image processing, three-dimensional volumetric visualization and isosurface generation. The toolkit and its codebase can be easily used by practitioners and developers as it provides high level classes, extensive documentation along with examples. VTK also provide binding support for popular scripting language such as Tcl (Tool Command Language) and Python which facilitates its rapid development. The toolkit is created and supported by Kitware Inc. which provides technical and commercial support. VTK can handle various types of data such as image data (`vtkImageData`), unstructured grid (`vtkUnstructuredGrid`), structures grid (`vtkStructuredGrid`), rectilinear grid (`vtkRectilinear Grid`) and unstructured points (`vtkPolyData`) (Caban et al., 2007).

Visualization of computed tomography (CT) and magnetic resonance (MR) imaging data is best done using a structured or rectilinear grid while ultrasound data can be visualized better using unstructured grid. The visual representation of the underlying data is attained by the toolkit using a data flow approach. It is easy to see how medical imaging software are able to be developed rapidly Once the VTK architecture and pipeline are understood, it is not hard to understand the rapid development of medical imaging software and how it is able to do so. The conceptual overview of the VTK pipeline is shown in Figure 2.11. Source module is the place where data are read which can then be filtered by various library of filters available in VTK. A visual representation is then created using a mapper which can be interacted with and transformed using the actor

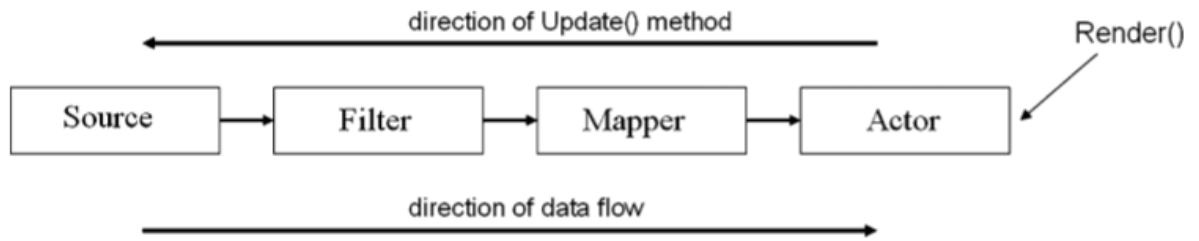


Figure 2. 11: Conceptual overview of the VTK pipeline

2.5.1. Image Processing in VTK

VTK supports multiple medical imaging techniques such as CT, MRI and ultrasound scans. The basic image processing and handling of image data is performed using a special data type (`vtkImageData`). The VTK allows rapid development of images due to its simplicity with Tcl binding to load, manipulate and visualize medical images. Other image processing capabilities of VTK includes image colouring based on prespecified color map (`vtkImageMapToColors`), histogram production and visualization (`vtkImageAccumulate`), Gaussian smoothing (`vtkImageGaussianSmooth`), image reslicing/ resampling from volume along an arbitrary axis (`vtkImageReslice`), appending images for volume creation (`VtkImageApped`), and extraction and visualization a region of interest (`vtkExtractVOI`).

2.5.2. Volume Rendering Using VTK

3D data visualization of CT and MR images are made possible through volume rendering. In volume rendering, simultaneous visualization of external and internal structure are made possible by assigning a colour and opacity values to each voxel. VTK pipeline is used as a mapper together with `vtkVolume` (which in this case replace `vtkActor`) for representing and interacting with the data. VTK provides two primary volume mappers to guarantee flexibility especially in terms of quality and speed. In order

to obtain image using ray casting, `vtkVolumeRayCastMapper` is used while texture mapping based on volume rendering is done using `vtkVolumeTextureMapper2D` as the mapper. Similar to `vtkActor`, the information regarding the orientation, position and scaling of data within a scene is contained in the `vtkVolume`. Additionally, parameters such as opacity and colours affecting the data's appearance are represented by its attribute, `vtkVolumeProperty`.

This attribute is usually attached with a transfer function to specifically define the volume properties' appearance enabling the projection of opaque skulls, translucent skin and red vessels. The VTK volume rendering pipeline is depicted in **Figure 12.12**. It all starts with the data reader from which a transfer function would be utilized for opacity and colour intensity mapping. The classification used by the raycast function and the order of interpolation are defined by the composite function. Afterwards, all information from the composting function and reader are assembled using a mapper and send to `vtkVolume`, that renders the resultant volume onto the screen.

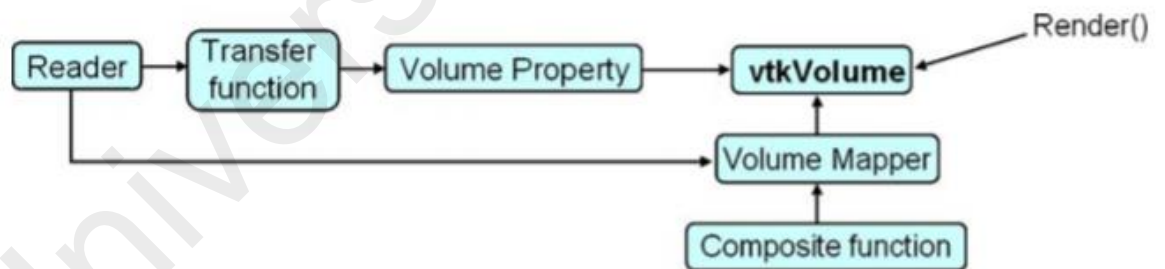


Figure 2. 12: Volume Rendering Pipeline Overview in VTK

2.5.3. Medical Applications of VTK

Several research has been conducted in the past on the medical application of VTK. A study by Hafizah et al. (2010) used VTK to reconstruct a 3D foetal model based on layers of 2D ultrasound images. The study compares the model created by using surface rendering technique through contour filtering and marching cube algorithm. The study concludes that marching cube algorithm gave a better result compared to contour filtering

as higher intensity 3D images can be generated thus enabling the viewer to easily detect the inner part and edges of the 3D model. The study also put emphasis on the need for noise removal using image processing technique. It also notes that the accuracy of the 3D image reconstructed can be improved by having a higher number of image slices used. The conclusion of this study is supported by Wang et al. (2009) which also shows superior reconstructed 3D model of a foot using the marching cube algorithm from CT scan images. A Study by Dong et al. (2013) used VTK for the reconstruction of the head and ankle. It found that varying the threshold allows the 3D image constructed to be clearer although the right threshold had to be determined manually. In a study by Choi et al. (2014), bone images were generated using the VTK software and it is found that the quality of the CT data is dictated by the opacity function. The study determined that the current practices was able to be optimized using VTK as the required number of steps are cut down. In a 2015 study, Yin and Lu were able to construct breast tumour 3D model using VTK. Various part of the breast can be discerned based on the area's intensity with improved detail using new technique for image segmentation.

Zhi et al. (2013) were able to construct a real-time vascular beating model through the mass-spring model using VTK. This allows doctors to evaluate how the vascular system are affected by physical forces which has potential application in intervention surgery. A study by Xiong et al. (2017) were able to use VTK to visualize the heart and coronary arteries, visualize the heart function as well as the myocardial perfusion in addition to visualizing the simulated coronary hemodynamic. The result of the research was deemed by cardiologist to have practical utility in the diagnosis of ischaemic heart disease. Interestingly, in 2011, Mc Farlene et al. used VTK to visualize and simulate surgery of the left ventricle. They were able to simulate the cutting, stitching and patching involved in heart restoration surgery as well as simulating the elastic deformation of the ventricle post operation. The research forms part of the virtual pathological heart of the Virtual

Physiological Human (VPH2) project developed under the European Commission Virtual Physiological Human (VPH) programme. More recently, Strocchi et al. (2020) were able to create models of four chamber hearts from a cohort of 24 heart failure patients which were used for cardiac electromechanics simulations.

2.6. 3D Slicer

3D Slicer (or just Slicer for short) is a free and open-source software developed to facilitate flexible biomedical and radiological medical imaging. It is a highly extensible medical image processing, visualization and analysis application platform originating in 1998 incredibly from a master thesis project between the surgical planning laboratory of Boston's Brigham and Women's Hospital and the Massachusetts Institute of Technology (MIT) Artificial Intelligence Laboratory. The initial aim was to develop a visualization and analysis software that is easy to use. First proposed by David Gering for his master's thesis, Slicer was then further developed by Steve Piper as its chief architect who commercialize its development effort in order to meet the industrial-scale installation packages requirement (Chang et al., 2019).

Slicer development was then further developed as a collaboration between GE global research institute, Isomics Company as well as Kitware, the same developer for VTK. The growing Slicer community also helps to contribute towards its development. Originally conceived as a system to guide neurosurgical therapy, visualization analysis, slicer had since become an all-embracing platform for clinical and preclinical research applications as well as non-medical image analysis such as CT scan image of mummies (Fedorov et al., 2012).

The development of slicer and its maintenance are funded by national institute of health and is further supported by its massive community of developers which

continuously propose solutions to problems and developed new tools for its continuous improvement. The main advantage of Slicer are its broad functionality, platform independence, good scalability and unlimited software licensing that are unrivalled by any other commercial and open source software tools with slicer like functionality (Zhang et al., 2019).

Other software may not be as easy to use, may require specialized hardware and are often expensive in comparison. Slicer also supports all the major operating system such as Windows, Linux and Mac OS X, ensuring its versatility in all applications (Chang et al., 2019).

2.7. Analysis of the Cardiac Chamber

Heart disease is the leading cause of death worldwide. Therefore, it is in the interest of the public for radiologist to increase their knowledge regarding the CT's cardiac chamber assessment for dedicated cardiovascular and conventional thoracic imaging protocols. This will improve the clinical usefulness of their imaging reports and medical consultations. Although most CT scan analysis can be performed using the conventional axial, sagittal and coronal planes views, they are still not enough for a full cardiac evaluation. Basic understanding of cardiac anatomy is required to analyse the cross-sectional imaging of the cardiac chambers. Standardized cardiac imaging planes includes the two-chamber, three-chamber as well as the four-chamber views which can be used for the assessment of cardiac morphology, function and size. These standardized imaging planes are common across various tomographic imaging modalities (Zezo, 2020).

2.7.1. Two-Chamber Views

The left ventricle's vertical long-axis is acquired from a plane passing through the centre of the mitral valve and the left ventricular apex in parallel to the middle portion of the interventricular septum. This view gives an overview of the left atrium, left ventricle and the mitral valve. It is a good view for analysing ventricular function especially at the inferior and anterior walls. This view can be utilized for evaluation of mitral valve morphology and function as well as the evaluation of the morphology, size and function for the left atrial and left ventricular chamber (Willems & Hazewinkel, 2009).

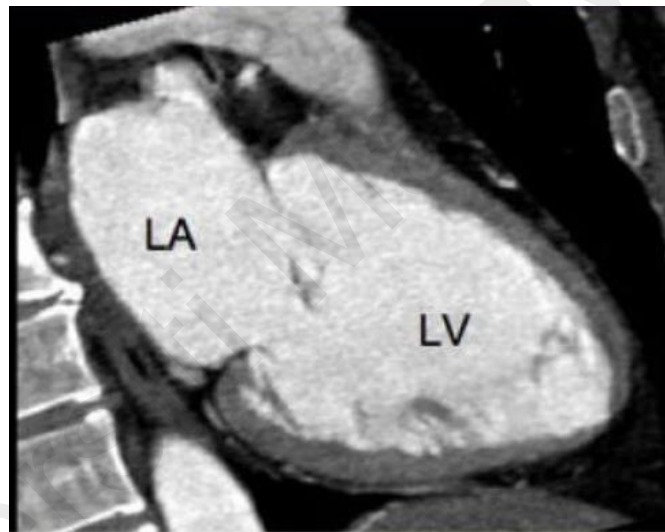


Figure 2. 13: 2-Chamber view. LA = left atrium, LV = left ventricle

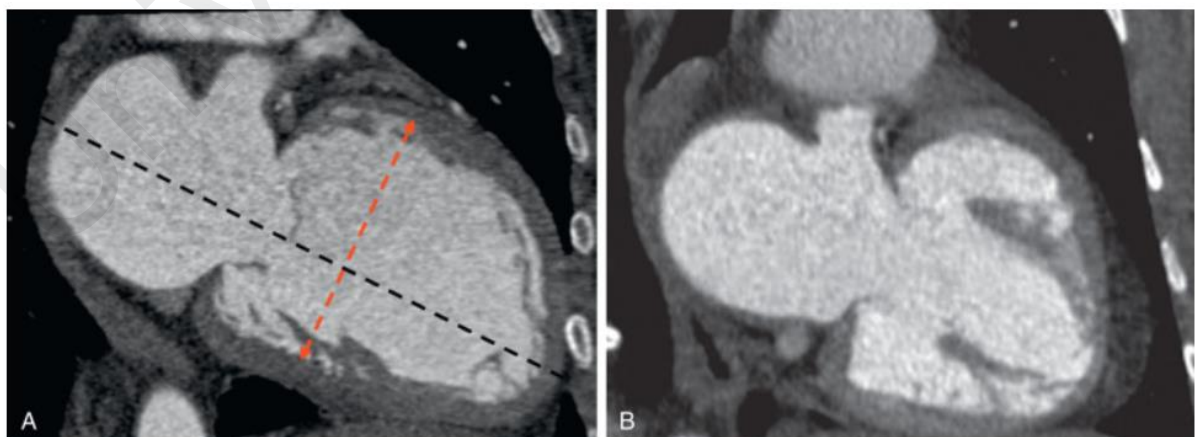


Figure 2. 14: Medical conditions depicted using the two-chamber view. (A) Left ventricular chamber dilation caused by dilated cardiomyopathy. (B) Isolated left ventricular hypoplasia.

2.7.2. Three-Chamber View

The three-chamber view is acquired from a plane which includes the long axis of the left ventricle and the centre line passing through the aortic root as well as the left ventricular outflow tract. In this view, the left atrium, left ventricle, aortic-, mitral valves and proximal aorta ascendens are visible. This view allows the evaluation of the left ventricular outflow tract morphology, mitral valve morphology and function, left ventricular inferolateral and anteroseptal walls as well as the aortic morphology, function and size (Koo et al., 2018).



Figure 2. 15: 3-Chamber view. LA = Left Atrium, Ao = aorta, LV = Left Ventricle

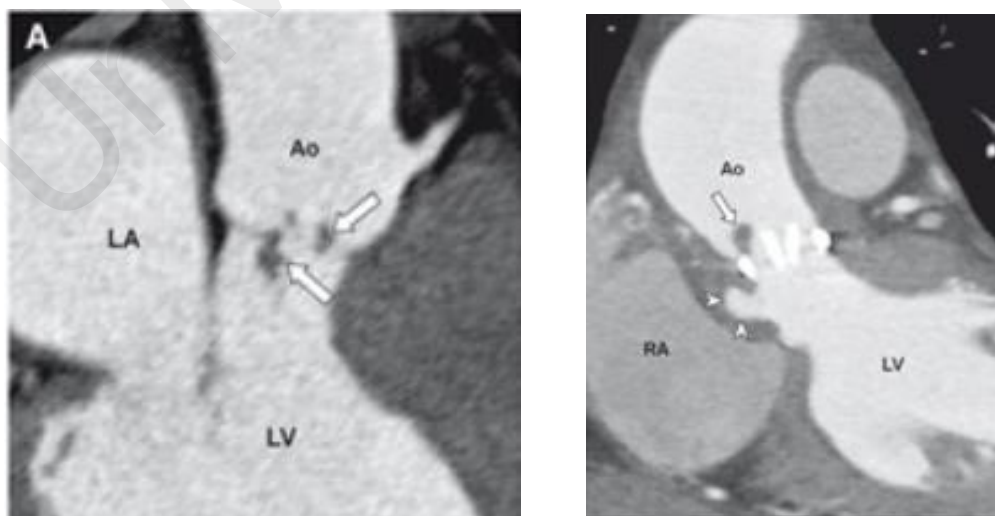


Figure 2. 16: Pathologies depicted through three-chamber view. (A) Low density vegetation on the right and left coronary cups in patient with infective endocarditis. (B) Paravalvular pseudoaneurysm (arrowheads) and small vegetation (arrow).

2.7.3. Four-Chamber View

The four-chamber view is acquired through a plane that slice through along the horizontal plane. Among the structures visible are the mitral valve as well as the tricuspid valves (with good contrast agent). The four-chamber view can be utilized for the evaluation of cardiac chamber morphology, interatrial and interventricular septum morphology, left ventricular lateral wall, left ventricular septal wall, right ventricular free wall as well as the pericardium (Ginat et al., 2011).

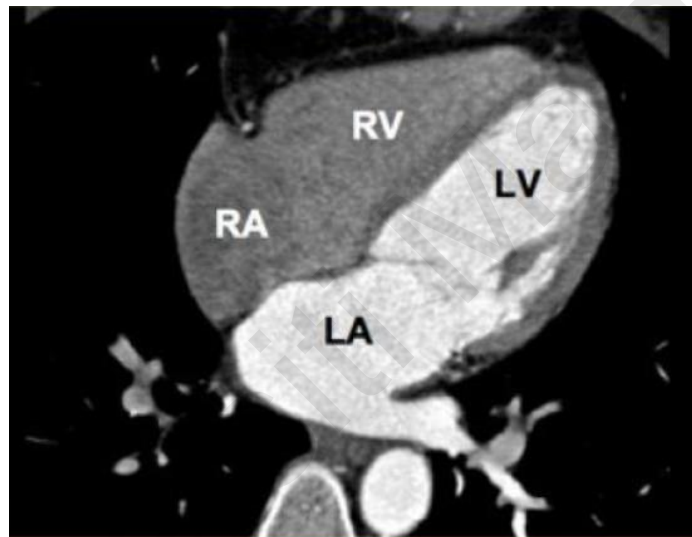


Figure 2.17: 4-chamber view. LA = left atrium, LV = left ventricle, RA = right atrium, RV = right ventricle.

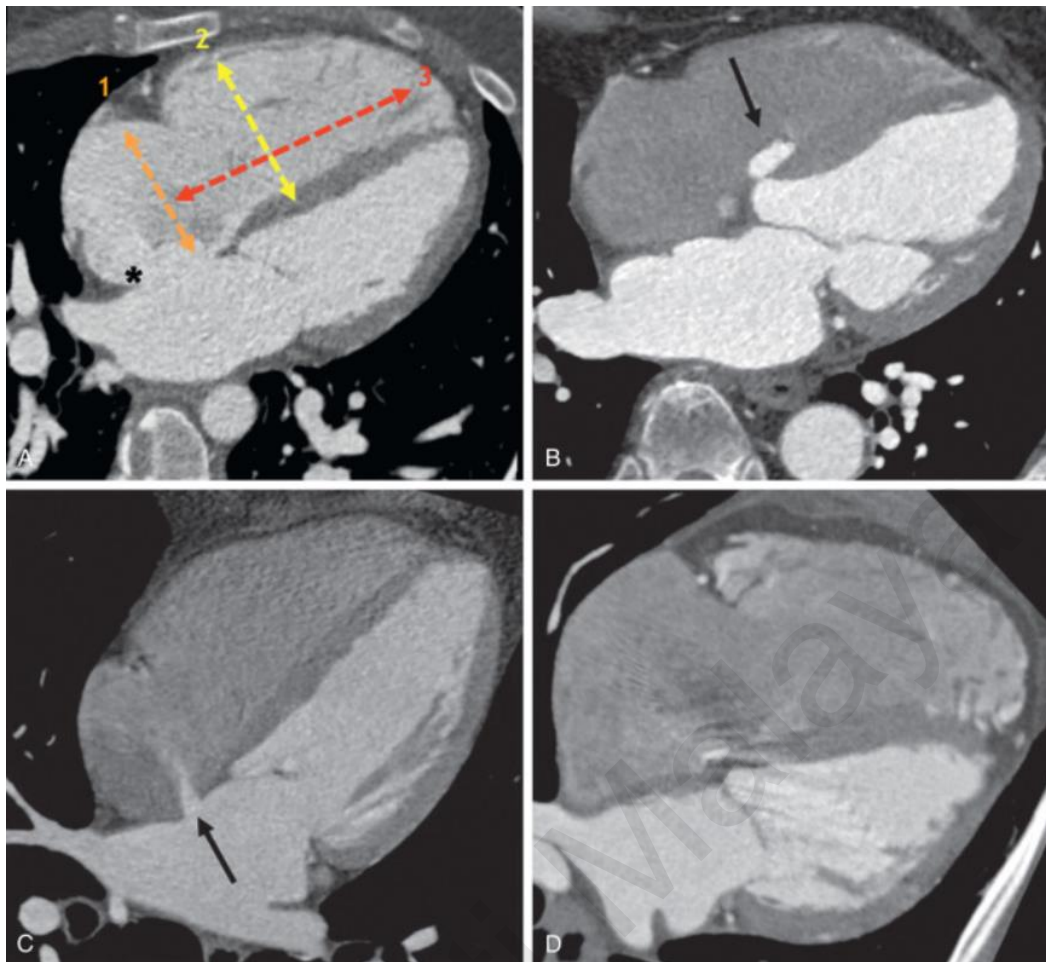


Figure 2. 18: Medical conditions depicted through the four-chamber view. (A) Dilation of the right ventricle (RV) caused by atrial septal defect (asterisks). 1. Basal RV diameter, 2. Mid-RV diameter, 3. RV length from base to apex. (B) Membranous ventricular septal aneurysm (arrow). (C) Patent foramen ovale with a left-to right shunt (arrow). (D) Dilation of RV chamber caused by arrhythmogenic RV dysplasia.

CHAPTER 3: METHODOLOGY

The data set chosen for this project involves 399 images originally in the DICOM format. It was originally taken in RSUP dr Hasan Sadikin, Bandung on 12th of November 2012 as part of a cardiac angiogram procedure using Computed Tomography (CT) scan of a female patient. The CT scan images were obtained with the help of a contrast agent. The cardiac angiogram performed suggested that the patient is suspected to have blockage or restriction of blood flow inside the blood vessels going to the heart. The first CT scan image is captured at position 1091.6mm along the axial direction, followed by another 398 images, ending at the 399th image at 972.2mm position.

The DICOM image would then be converted into JPEG images using the MicroDICOM software reducing the image bits from 12 bits to 8 bits. The images were then converted into gray scale and the image noises were reduced using Photoshop's noise reduction filter to provide clearer and crisper images. The CombineA9 measureDistance program template was primarily used as the source code for the generation of the 3D images. Several coding lines particularly with regards to opacity and colour were changed to generate the desired image. The generated 3D images were manipulated by slicing the heart at different planes and angles. This enables the heart to be viewed in several section views including the axial view, sagittal view, coronal view, 2-Chamber view, 3-Chamber view and 4-Chamber view. The different plane views stated provide a comprehensive view of the heart and its inner chamber thereby facilitating the detection of any anomalies which can be referred to for preventive action and treatment decisions.

The acquisition and reconstruction of 3D images are done following several steps. The software used in this paper is visualization toolkit (VTK).

3.1. 2D CT Image Acquisitions.

The images used in this paper are CT images. There are 399 layers of 2D images used for the reconstruction of 3D images. The output resolution of the 3D reconstructed image is 512 x 512.

3.2. Volume Rendering Process

The function `vtkJPEGReader` in VTK would be used to convert all the image slices into a volumetric display. The volume rendering process in this paper follows the pipeline shown in **Figure 3.1**.

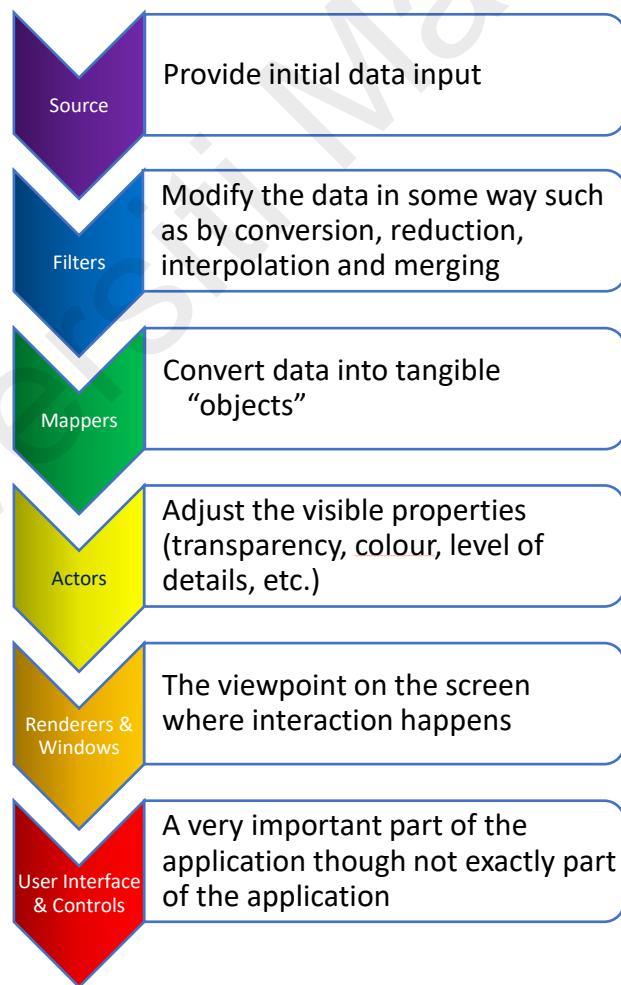


Figure 3. 1: VTK Visualization Pipeline

a. Sources/Reader

The initial data input can be obtained from various sources. Put it simply, source are basically the origin of the data flowing through the visualization pipeline. In this case, the sources are multiple 2D CT scan images of the heart. The reader used is “vtkJPEGReader”.

b. Filter

Filters are the VTK components which received data from other components as an input, modified it in some way, before delivering the modified output data to be used by other components. Some portion of a large data set might be extracted using filters which can also extract sub-sample data sets to coarser resolution, interpolate data set to a finer resolution, merging multiple input into a combined output, split compound input into its component parts as well as some other numerous varieties of transformations. The filters can be used to select the size, strength and intensity of the data, to process the 2D/3D images and to create geometrical objects from the data utilized.

c. Mappers

Mappers received data from other VTK components (either from filters or sometimes directly from the source) and map it to a form of physical manifestation (graphics primitives such as points, lines or triangles) that can be rendered and displayed by the rendering engine. The mapper used in this study is vtkPolyDataMapper which maps the 2D CT scan images to the graphics primitives.

d. Actors

The objects' geometry and properties in a rendering scene is represented by the `vtkActor`. Actors allowed the appearance properties of the physical manifestations of data to be adjusted and controlled as rendered onto the screen. It has position, texture, orientation, scale and various rendering properties. Some of the properties typically controlled using actors are transparency and colour mapping. It also keeps a reference to the mapper.

e. Rendering

Rendering converts 3D graphics primitives (Such as points, lines, triangles), materials and lights specifications as well as camera view into a 2D image that can be displayed on the screen. It carries out coordinate transformation between world coordinates, view coordinates and display coordinates. The renderer used in this study is `vtkRenderer` and it controls the rendering process for actors and scenes. In this stage, the render window background colour can also be set.

f. Render Window

The `vtkRenderWindow` used in this study creates a window for which the renderers can draw into so that the final 3D model can be displayed. It is basically what users would actually see on the screen.

g. Interactors

The `vtkRenderWindow Interactor` allows platform independent window interaction using mouse and keyboard. It also enables the rotation, panning and zooming of the camera when viewing the 3D images as well as selecting and manipulating the actors. Time events are also handled by the interactors.

3.3. Coding

This section explains the coding utilized and its effects on the reconstructed 3D cardiac chamber image. Different kind of coding is utilized to get different visualized image. The first coding reads a volume dataset to create a volumetric display using volume rendering technique while the second coding construct 3D image using surface rendering technique. The following coding performs multiplanar rendering by creating three orthogonal planes while the last coding enables the observation of reconstructed 3D images' cross-sectional views in different planes. The last coding also allows the measurement between two points inside the heart chamber.

3.3.1. Volume Rendering of the 2D CT-Scan Cardiac Images

As mentioned in previous section regarding the pipeline mechanism, a reader should first be defined. In this study, the reader used is vtkJPEGReader. The following lines of coding used allows a series of 2D slice images to be read which would then be combined to create a volumetric model. The slice dimensions are set using SetDataExtent where the size of pixel in the x direction is set at 512 while the size in the y direction is set at 512. The number of image layers used, 399 is set for the Z direction for the reconstruction of a 3D image.

```
vtkJPEGReader *reader = vtkJPEGReader::New();
reader->SetDataExtent(0,511,0,511,1,399);
reader->SetFilePrefix("C:\\Users\\User\\Desktop\\Medical image 2\\JPEG
Noise Reduced\\img");
reader->SetFilePattern("%s%d.jpg");
reader->SetDataSpacing(1, 1, 0.98);
reader->SetDataOrigin(0.0, 0.0, 0.0);
reader->Update();
```

Filter is then applied to allow the relevant 3D image to be rendered and to disable irrelevant image from obscuring the intended image of interest. The chosen opacity values are stated below which allows the chamber of the heart to be visible and visualized.

```
vtkPiecewiseFunction *opacityTransferFunction =
vtkPiecewiseFunction::New();
    opacityTransferFunction->AddPoint(1024+0, 0.0);
    opacityTransferFunction->AddPoint(1024+80, 0.5);
    opacityTransferFunction->AddPoint(1024+140, 0.0);
    opacityTransferFunction->AddPoint(1024+200,0.0);
```

Next, vtkColorTransferFunction is used to give colours to each layers of rendered image. Suitable RGB point value is used to provide contrast between the different types of tissues inside and around the heart to give a good image. Setpoint 1024+0 was identified to be the epithelial layer of the heart and body outer skin. Setpoints from 1024+80 was set to be the muscle of the heart and the color chosen was in red. Blue color was chosen at set point 1024+130 to produce a “marker” like effect in the interior wall of the left atrium and left ventricle. Setpoint 1024+200 represents the bone tissue, cavity in the aorta and the inner cavity of left ventricle and left atrium. The opacity was set to 0.00 to produce an empty volume in the inner cavities of the left ventricle, left atrium and aorta so that medical practitioners can observe inner structures for abnormalities.

```
vtkColorTransferFunction *colorTransferFunction =
vtkColorTransferFunction::New();
    colorTransferFunction->AddRGBPoint(1024+0, 0.9, 0.9, 0.7);
    colorTransferFunction->AddRGBPoint(1024+80, 1, 0, 0);
    colorTransferFunction->AddRGBPoint(1024+130, 0, 0, 1);
```

The properties of the volume rendering is represented using vtkVolumeProperty. The brightness of the surrounding image of the cardiac can be adjusted using the SetAmbient function. SetDiffuse performs similar function. SetSpecular controls the lighting of the render window with a larger value giving off a brighter lighting. SetSpecularPower acts

like a mirror in which a larger value result in darker image rendered though with much better image contrast.

```
vtkVolumeProperty *volumeProperty = vtkVolumeProperty::New();
volumeProperty->SetColor(colorTransferFunction);
volumeProperty->SetScalarOpacity(opacityTransferFunction);
volumeProperty->ShadeOn();
volumeProperty->SetInterpolationTypeToLinear();
volumeProperty->SetAmbient(0.1);
volumeProperty->SetDiffuse(0.9);
volumeProperty->SetSpecular(0.9);
volumeProperty->SetSpecularPower(40);
```

3D image is generated through the volume rendering process using VtkVolumeRayCastMapper where light changes that went through the 3D volume data is projected as the visualization output results.

```
vtkVolumeRayCastCompositeFunction *compositeFunction =
vtkVolumeRayCastCompositeFunction::New();
```

The plane for cross sectional view of the cardiac image can be displayed using vtjPlane.

```
vtkPlane *plane=vtkPlane::New();

vtkVolumeRayCastMapper *volumeMapper = vtkVolumeRayCastMapper::New();
    volumeMapper->SetVolumeRayCastFunction(compositeFunction);
    volumeMapper->SetInputConnection(readerImageCast-
>GetOutputPort());
    volumeMapper->AddClippingPlane(plane);
volume = vtkVolume::New();
    volume->SetMapper(volumeMapper);
    volume->SetProperty(volumeProperty);
    volume->PickableOff ();
```

Filter would then be applied to create an outline of a box whereby the 3D image would be rendered and visualized in. The colour of the outline can be set based on the RGB value.

```
vtkOutlineFilter *outline = vtkOutlineFilter::New();
    outline->SetInputConnection( readerImageCast->GetOutputPort() );
vtkPolyDataMapper *outlinemapper = vtkPolyDataMapper::New();
```

```

        outlineMapper->SetInputConnection( outline->GetOutputPort() );
vtkActor * outlineActor = vtkActor::New();
        outlineActor->SetMapper( outlineMapper );
        outlineActor->GetProperty()->SetColor( 0.5, 0.5, 1);

```

VtkSphereSource is used to create a sphere that function as a point whereby the image can be click and manipulate at. The SetDiffuseColor function can be used to change the color of the sphere based on the RGB vale. R=0.5,0.5,0.5 for example will create a dark greyish white coloured sphere.

```

vtkSphereSource *sphere1 = vtkSphereSource::New();
        sphere1->SetRadius(30);
vtkPolyDataMapper *sphereMapper1 = vtkPolyDataMapper::New();
        sphereMapper1->SetInput( sphere1->GetOutput() );
        sphereMapper1->GlobalImmediateModeRenderingOn();
sphereActor1 = vtkActor::New();
        sphereActor1->SetMapper( sphereMapper1 );
        sphereActor1->GetProperty()->SetDiffuseColor(0.5,0.5,0.5);

```

The setting and colour for the second sphere can also be adjusted based on the coding below.

```

vtkSphereSource *sphere2 = vtkSphereSource::New();
        sphere2->SetRadius(30);
vtkPolyDataMapper *sphereMapper2 = vtkPolyDataMapper::New();
        sphereMapper2->SetInput( sphere2->GetOutput() );
        sphereMapper2->GlobalImmediateModeRenderingOn();
sphereActor2 = vtkActor::New();
        sphereActor2->SetMapper( sphereMapper2 );
        sphereActor2->GetProperty()->SetDiffuseColor(1,0.5,0.5);

```

After the two sphere points are created, a line between the two spheres is generated whereby the resolution and the colour can be set. In this example the resolution is set at 200 with the RGB colour of (0,1,0) representing green colour.

```

line=vtkLineSource::New();
        line->SetPoint1(0, 0, 0.5);
        line->SetPoint2(0, 0, 0);
        line->SetResolution(200);
vtkPolyDataMapper *lineMapper = vtkPolyDataMapper::New();
        lineMapper->SetInput(line->GetOutput());
lineActor = vtkActor::New();
        lineActor->SetMapper(lineMapper);
        lineActor->GetProperty()->SetDiffuseColor(0,1,0);

```

vtkCellPicker selects a cell by shooting a ray into graphics window which will intersect with the defining geometry of the actor thus specifying the cells. This will return the coordinates, actor and mapper as well as the id of the closest cell within the tolerance of the pick ray for which the dataset would then be picked.

```
PickCommand* pickObserver = PickCommand::New();
    picker = vtkCellPicker::New();
    picker->AddObserver( vtkCommand::EndPickEvent, pickObserver );
```

vtKTextMapper allows what the operator has picked to be displayed in the render window. VTK allows the properties of the text to be set using the tprop. SetFrontFamilyArial will set the text font to Arial. The text size can be adjusted using the SetFontSize (x) function, whereby x here is the desired text size. The SetColor function sets the colour of the text based on the RGB value input.

```
textMapper = vtkTextMapper::New();
    vtkTextProperty *tprop = textMapper->GetTextProperty();
    tprop->SetFontFamilyToArial();
    tprop->SetFontSize(20);
    tprop->BoldOn();
    tprop->SetColor(1, 0, 0);
    textActor = vtkActor2D::New();
    textActor->VisibilityOff();
    textActor->SetMapper(textMapper);
```

Lastly, the usage of mouse and keyboard for controlling the camera and viewpoint of the 3D rendered image are enabled using the vtkInteractorStyleTrackball Camera function.

```
vtkInteractorStyleTrackballCamera *style =
    vtkInteractorStyleTrackballCamera::New();
    vtkCallbackCommand * pickerCommand = vtkCallbackCommand::New();
    pickerCommand->SetClientData(style);
    pickerCommand->SetCallback(PickerInteractionCallback);
    style->AddObserver(vtkCommand::LeftButtonPressEvent,
pickerCommand);
    style->AddObserver(vtkCommand::MouseMoveEvent, pickerCommand);
    style->AddObserver(vtkCommand::LeftButtonReleaseEvent,
pickerCommand);
    style->AddObserver(vtkCommand::RightButtonPressEvent,
pickerCommand);
```



```

    iren->SetInteractorStyle(style);
    iren->SetPicker(picker);

    sphereActor1->VisibilityOff();
    sphereActor2->VisibilityOff();
    lineActor->VisibilityOff();

    vtkTIPWCallback *myCallback = vtkTIPWCallback::New();
    myCallback->Plane = plane;
    myCallback->Volume = volume;

    vtkImplicitPlaneWidget *planeWidget = vtkImplicitPlaneWidget::New();
    planeWidget->SetInteractor(iren);
    planeWidget->SetPlaceFactor(1.25);
    planeWidget->GetPlaneProperty()->SetOpacity ( 0.1 );
    planeWidget->GetOutlineProperty()->SetColor(0,0,1);
    planeWidget->SetOrigin(xx/2,yy/2,zz/2);
    planeWidget->SetInput((vtkDataSet *)readerImageCast->GetOutput());
    planeWidget->PlaceWidget();
    planeWidget->On();
    planeWidget->AddObserver(vtkCommand::InteractionEvent,myCallback);

    vtkCamera *cam1 = ren1->GetActiveCamera();
    cam1->Zoom(1.5);

```

The background colour and the size of the render window can also be adjusted by using the `SetSize` function. The visibility of the plane can be turn on and off using the `SetKeyCode ('i')` function.

```

ren1->AddVolume(volume);
ren1->AddActor(sphereActor1);
ren1->AddActor(sphereActor2);
ren1->AddActor(lineActor);
ren1->AddActor2D(textActor);
ren1->AddActor( outlineactor );
ren1->SetBackground(1, 1, 1);
renWin->SetSize(600, 600);
renWin->Render();
iren-> SetDesiredUpdateRate(99);
iren->SetKeyCode('i');

```

3.3.2. Surface Rendering of the Heart Chamber

Similar to what is applied during volume rendering, surface rendering also made use of JPEGReader to read the JPEG images.

```
vtkJPEGReader *v16 = vtkJPEGReader::New();

v16->SetDataExtent(0,511,0,511,0,200);
v16->SetFilePrefix("C:\\Users\\User\\Desktop\\Medical image 2\\JPEG
Noise Reduced\\img");
v16->SetFilePattern("%s%d.jpg");
v16->SetDataSpacing(1, 1, 1.2);
v16->SetDataOrigin(0.0, 0.0, 0.0);
v16->Update();
```

vtkPolyDataNormals is used for rendering surface shading.

```
vtkSmartPointer<vtkContourFilter> skinExtractor =
    vtkSmartPointer<vtkContourFilter>::New();
skinExtractor->SetInputConnection(v16->GetOutputPort());
skinExtractor->SetValue(0, 10);

vtkSmartPointer<vtkPolyDataNormals> skinNormals =
    vtkSmartPointer<vtkPolyDataNormals>::New();
skinNormals->SetInputConnection(skinExtractor->GetOutputPort());
skinNormals->SetFeatureAngle(60.0);

vtkSmartPointer<vtkStripper> skinStripper =
    vtkSmartPointer<vtkStripper>::New();
skinStripper->SetInputConnection(skinNormals->GetOutputPort());

vtkSmartPointer<vtkPolyDataMapper> skinMapper =
    vtkSmartPointer<vtkPolyDataMapper>::New();
skinMapper->SetInputConnection(skinStripper->GetOutputPort());
skinMapper->ScalarVisibilityOff();
```

SetDiffuseColor is used to change the colour of the skin by assigning the RGB values.

In general, a red colour is desired when rendering the skin surface of the heart.

```
vtkSmartPointer<vtkActor> skin =
    vtkSmartPointer<vtkActor>::New();
skin->SetMapper(skinMapper);
skin->GetProperty()->SetDiffuseColor(1, .49, .25);
skin->GetProperty()->SetSpecular(.3);
skin->GetProperty()->SetSpecularPower(20);
skin->GetProperty()->SetOpacity(1);
```

The colour of the bones can also be assigned using a similar line of coding.

```

vtkSmartPointer<vtkContourFilter> boneExtractor =
    vtkSmartPointer<vtkContourFilter>::New();
boneExtractor->SetInputConnection(vl6->GetOutputPort());
boneExtractor->SetValue(0, 230);

vtkSmartPointer<vtkPolyDataNormals> boneNormals =
    vtkSmartPointer<vtkPolyDataNormals>::New();
boneNormals->SetInputConnection(boneExtractor->GetOutputPort());
boneNormals->SetFeatureAngle(60.0);

vtkSmartPointer<vtkStripper> boneStripper =
    vtkSmartPointer<vtkStripper>::New();
boneStripper->SetInputConnection(boneNormals->GetOutputPort());

vtkSmartPointer<vtkPolyDataMapper> boneMapper =
    vtkSmartPointer<vtkPolyDataMapper>::New();
boneMapper->SetInputConnection(boneStripper->GetOutputPort());
boneMapper->ScalarVisibilityOff();

vtkSmartPointer<vtkActor> bone =
    vtkSmartPointer<vtkActor>::New();
bone->SetMapper(boneMapper);
bone->GetProperty()->SetDiffuseColor(0.4, 1, .9412);

```

3.3.3. Measuring Length between two points

VTK program allows the measurement between two points thus enabling the length, width and height of the heart structures to be determined. This requires that the length of one pixel to be defined. However, since the 2D CT image used is in the JPEG format instead of DICOM, the correct size of one pixel is not automatically assigned. The resolution for the 2D CT image used is 512 × 512. The default pixel size is given as 0.0054590294. Based on the DICOM tag, the reconstruction diameter is 156 mm. Therefore, a multiplication factor of 2.79 was added to the coding in order to get the correct pixel size that would result in the reconstruction diameter of 156 mm from 512 pixels.

```

double millimeter;
//millimeter=length * 0.0054590294;
millimeter=length * 0.0054590294 * 2 * 2.79;

char text[120];
sprintf( text, "The length of two points is %5.5f cm", millimeter);
textMapper->SetInput( text );

```

Accordingly, the data spacing in the z direction is given as 0.98

```

vtkJPEGReader *reader = vtkJPEGReader::New();
reader->SetDataExtent(0,511,0,511,1,399);
reader->SetFilePrefix("C:\\Users\\User\\Desktop\\Medical image 2\\JPEG
Noise Reduced\\img");
reader->SetFilePattern("%s%d.jpg");
reader->SetDataSpacing (1, 1, 0.98);
reader->SetDataOrigin(0.0, 0.0, 0.0);
reader->Update();

```

This setting allows the correct pixel size to be assigned for an accurate measurement between two points using VTK software.

3.4. 3D slicer

The DICOM files of the 399 CT scan images are loaded to the 3D slicer program. Pre-set CT-Cardiac was chosen as the default setting to display the 3D model as it is specialized in visualizing heart images. Rendering is done using VTK CPU Ray Casting. The Display ROI function is turned on so that it is easier to identify location of interest on the different planes that are displayed together. The Crop function is enabled to slice the 3D model of the heart in different planes at different layers in order to investigate the condition of the heart and identify anomalies. Measurements between two points are done using the ruler function whereby the distance between two points clicked are displayed.

CHAPTER 4: RESULTS

4.1. 3D Reconstruction of Cardiac Chamber Image

Figure 4.1 shows the general structure of the heart. Figure 4.2 shows the isometric view of the overall 3D model as visualized through the VTK program using the volume rendering method. The colour of the skin is set at RGB values of (0.9,0.9, 0.7) which produce a light brown colour while the colour of the heart muscle is set to be red. The colour gradient for the layers in between the two values produce a pinkish hue. The bone layer is turned off too to reduce the noise that will be produced in the aorta and inner cavity of the heart.

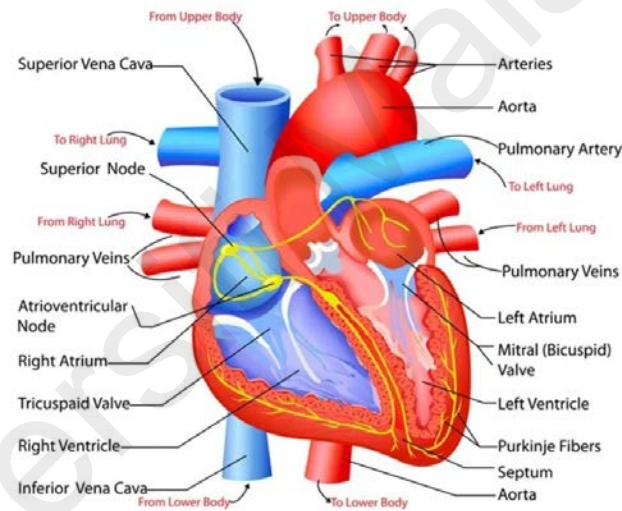


Figure 4. 1: General structure of the heart

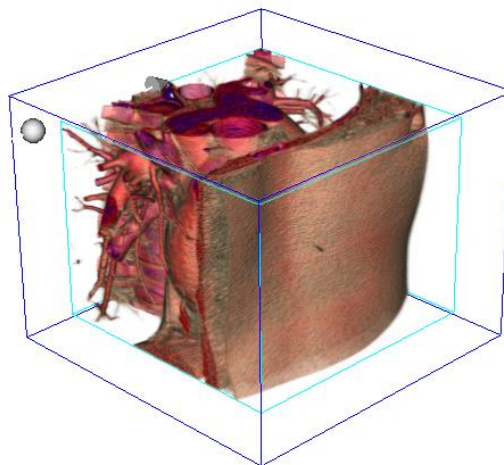


Figure 4. 2: Isometric view of the overall 3D model.

In this report, 6 sectional views of the heart were made using VTK program and they are presented as follows:

1) Axial View

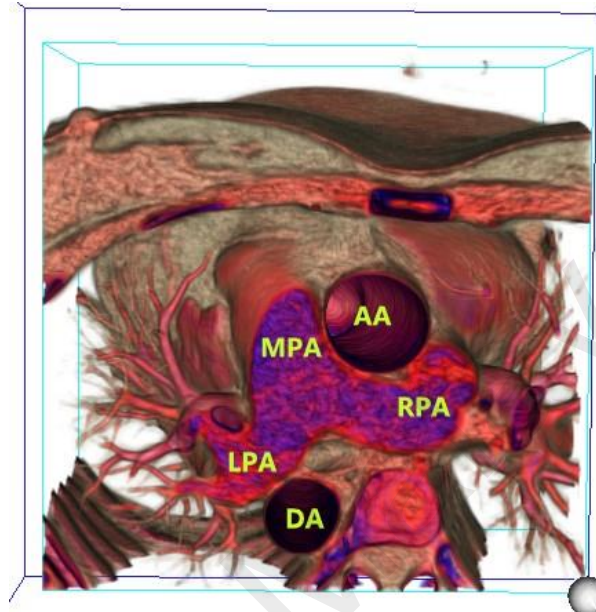


Figure 4. 3: Axial view of the heart. (DA-Descending Aorta, AA-Ascending Aorta, MPA-Main Pulmonary Artery, LPA-Left Pulmonary Artery and RPA-Right Pulmonary Artery).

2) Sagittal View

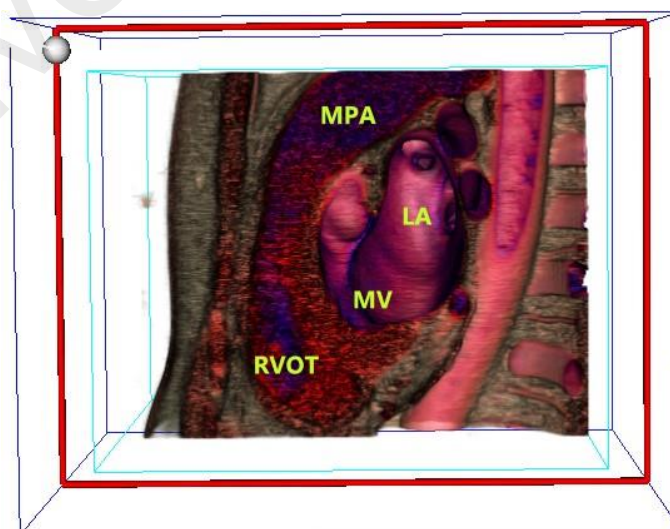


Figure 4. 4: Sagittal view of the heart. (MPA-Main Pulmonary Artery, RVOT-Right Ventricular Outflow Tract, LA-Left Atrium and MV-Mitral Valve).

3) *Coronal View*

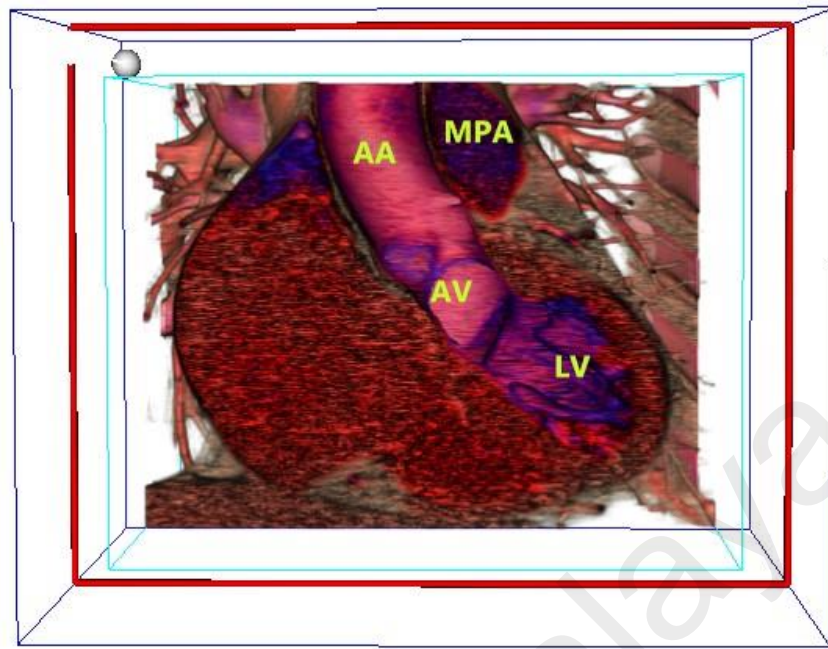


Figure 4. 5: Coronal view of the heart. (MPA-Main Pulmonary Artery, AA-Ascending Aorta, AV-Aortic Valve, and LV-Left Ventricle).

4) *2 Chamber View*

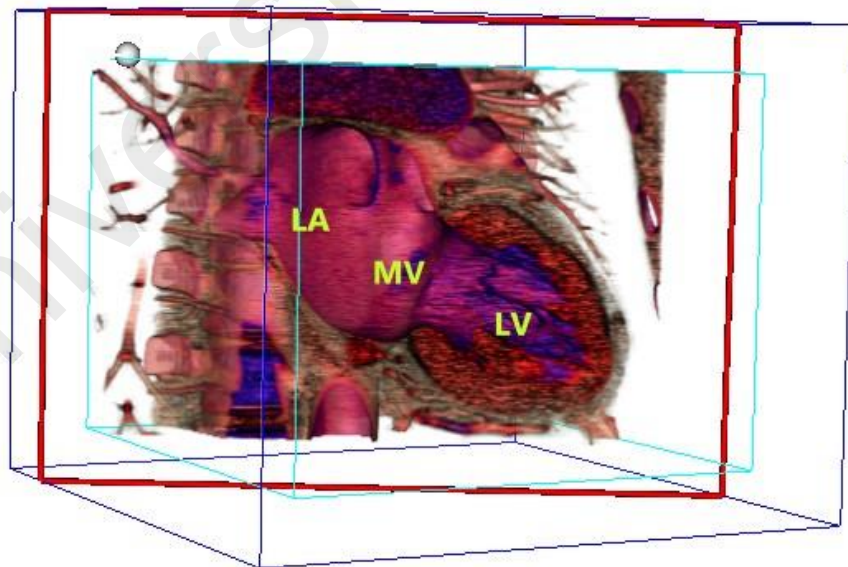


Figure 4. 6: Two chamber view of the heart. (LA-Left Atrium, MV-Mitral Valve and LV-Left Ventricle).

5) 3 Chamber View

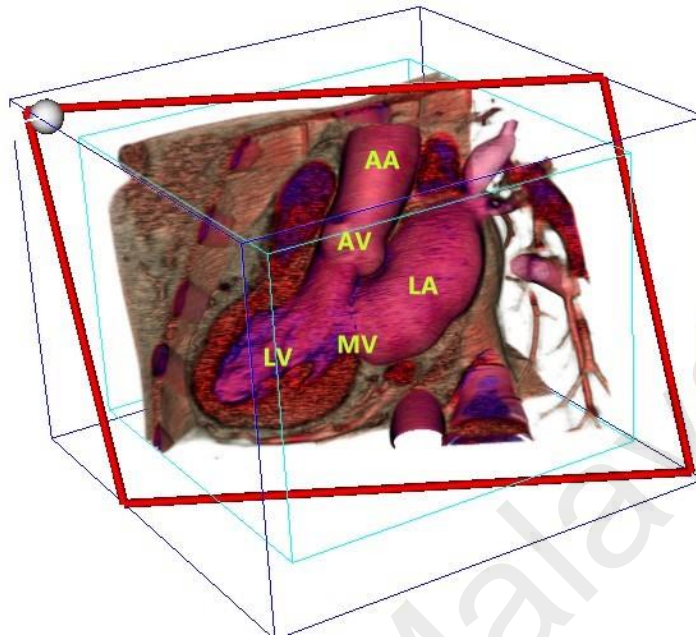


Figure 4. 7: Three chamber view of the heart. (LA-Left Atrium, MV-Mitral Valve, LV-Left Ventricle, AV-Aortic Valve and AA-Ascending Aorta).

6) 4 Chamber View

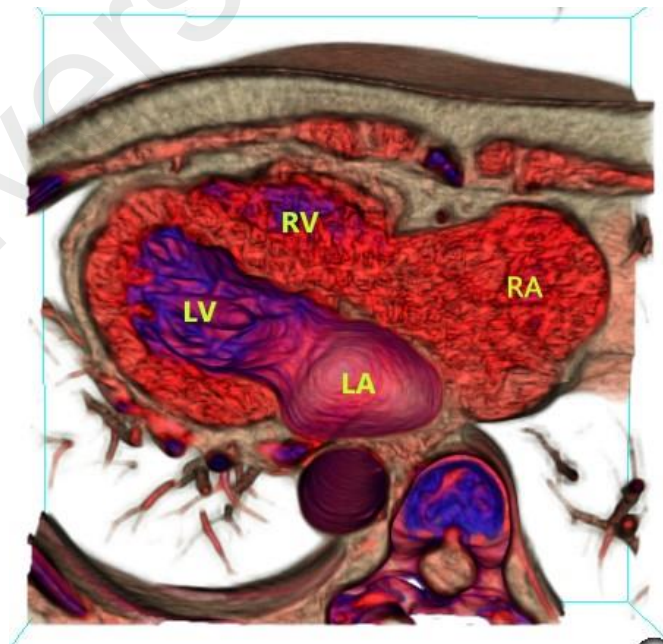


Figure 4. 8: Four chamber view of the heart. (LA-Left Atrium, LV-Left Ventricle, RA-Right Atrium and RV-Right Ventricle).

4.2. Comparison with Cardiac Chamber Image Reconstruction using 3D slicer

The reconstruction of the heart in 3D can be made possible using both VTK as well as 3D slicer using input in the DICOM as well as JPEG format. In 3D slicer, it is possible to view the 3D image together with its 2D counterparts in the axial, sagittal and coronal plane at the same time. When the region of interest (ROI) function is made visible, it is possible to pinpoint exactly the location of region of interest on the 3 planes for a more precise identification and confirmation of the object of interest (such as tumours, blockage and deformations).

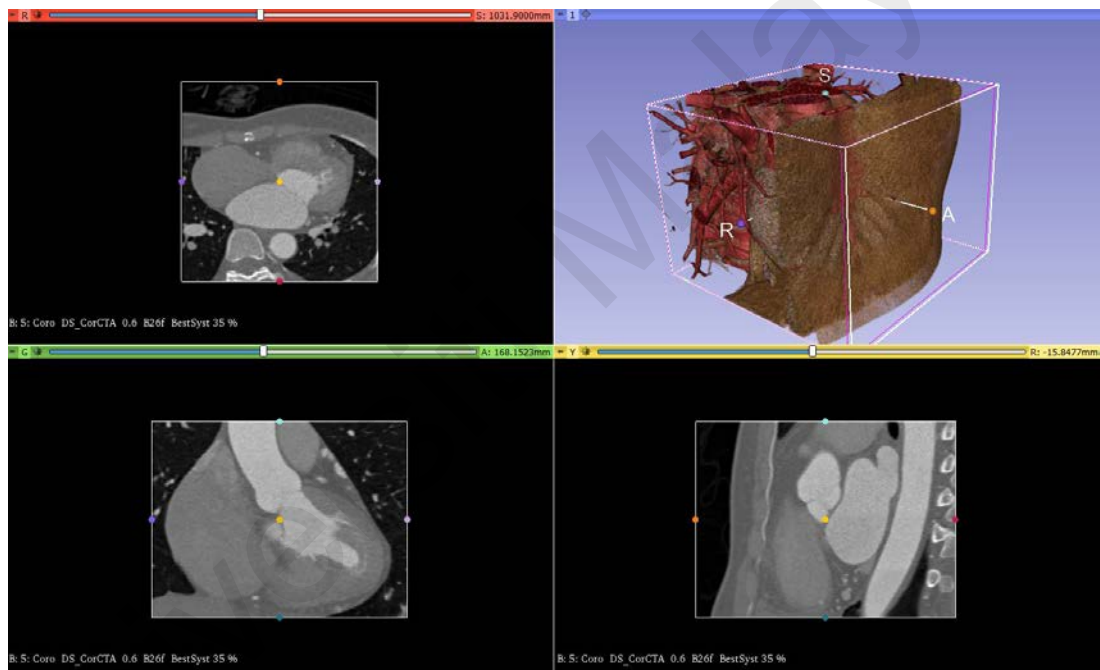


Figure 4. 9: Views of different planes generated on a single window using 3D Slicer

The opacity and RGB colour point values at different layers set point need to be assigned manually when using VTK while in 3D slicer, the operators are given multiple pre-set options from which the 3D model can be displayed with. The pre-set options are already specialized for visualizing different regions of the body thus enabling a quicker visualization of the object of interest. The 3D reconstructed image properties can be further adjusted in terms of opacity, colour as well as filters such as ambient, diffuse, specular and power.

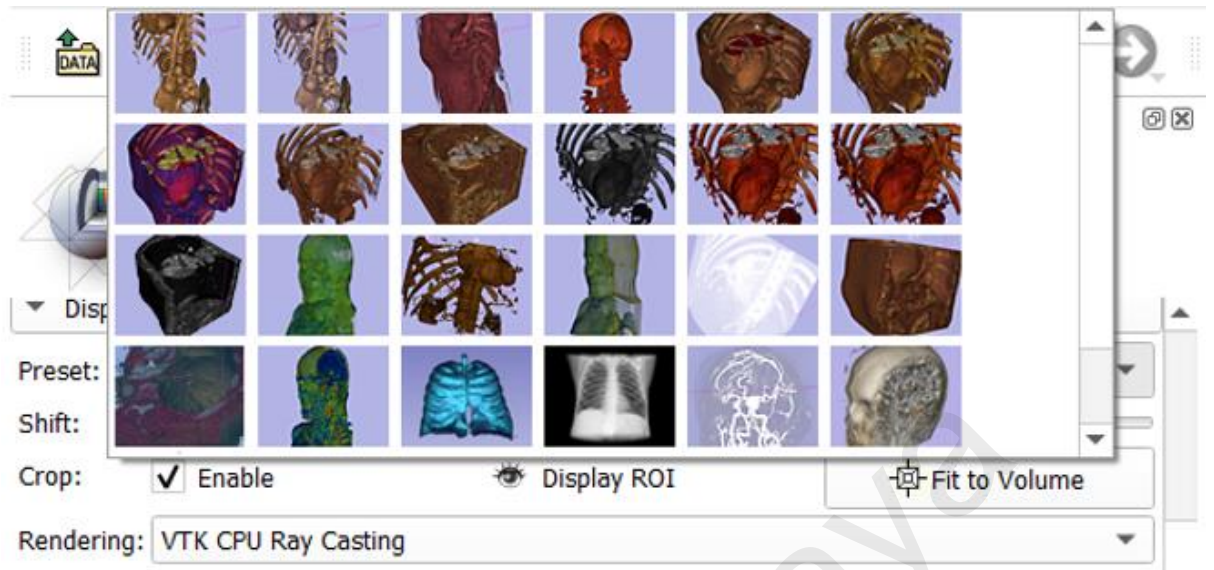


Figure 4. 10: Pre-set Options for Display of 3D Model using 3D slicer

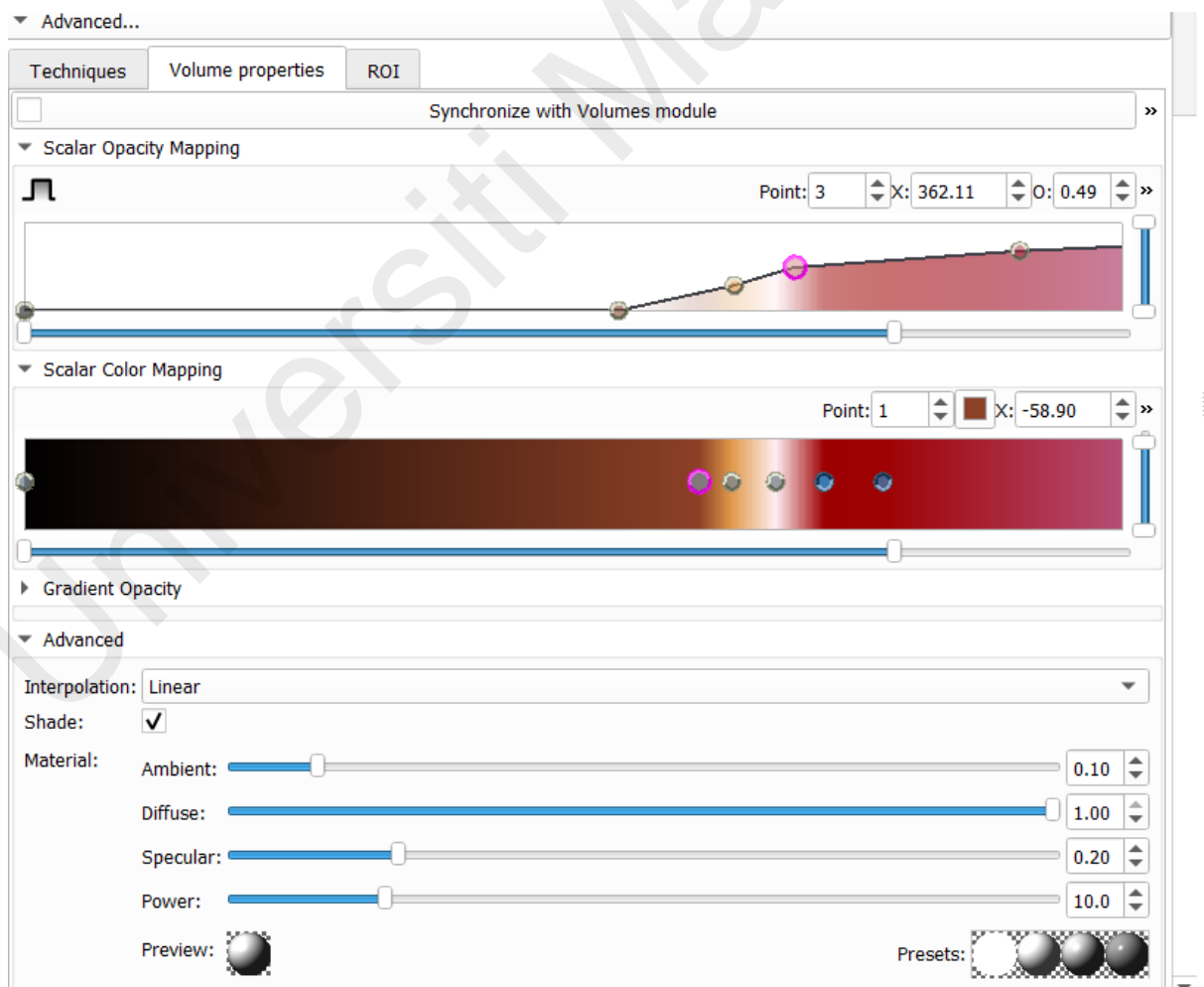


Figure 4. 11: Volume Properties Adjustment using 3D slicer

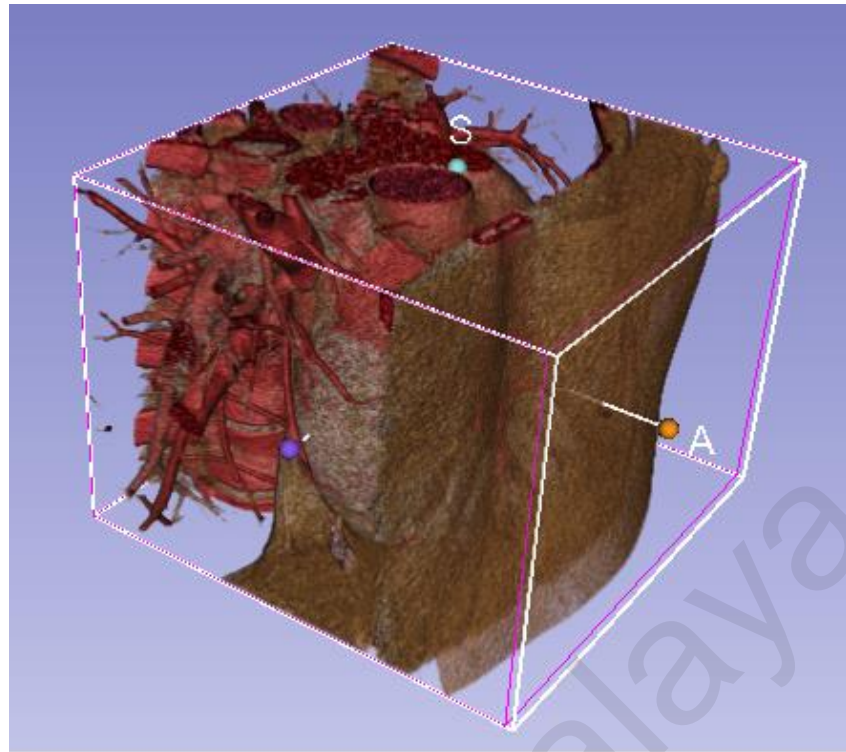


Figure 4. 12: Isometric view of the overall 3D model using 3D slicer

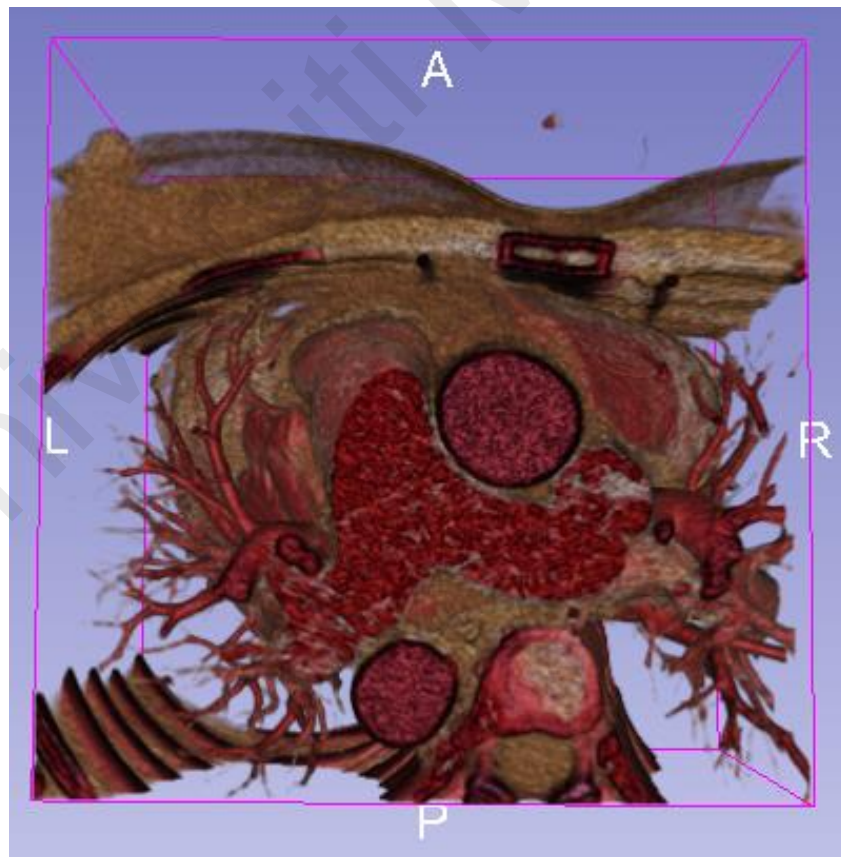


Figure 4. 13: Axial view of the heart using 3D slicer

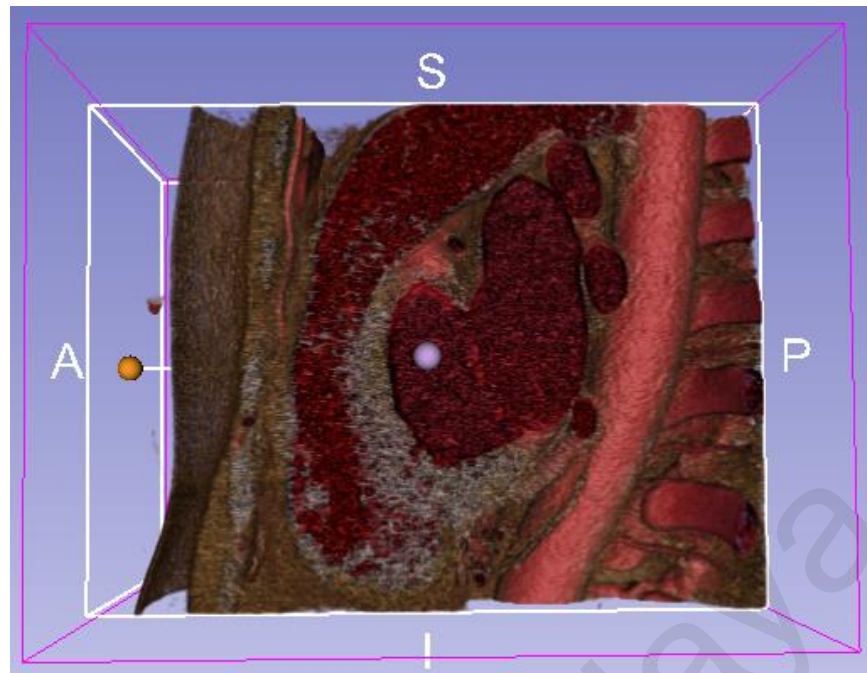


Figure 4. 14: Sagittal view of the heart using 3D slicer

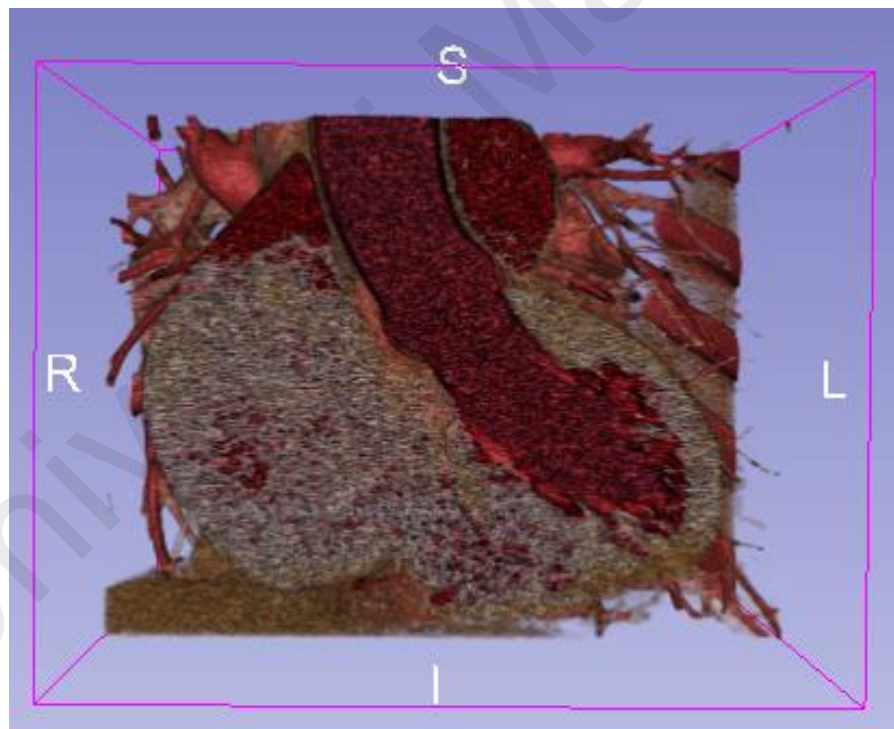


Figure 4. 15: Coronal view of the heart using 3D slicer

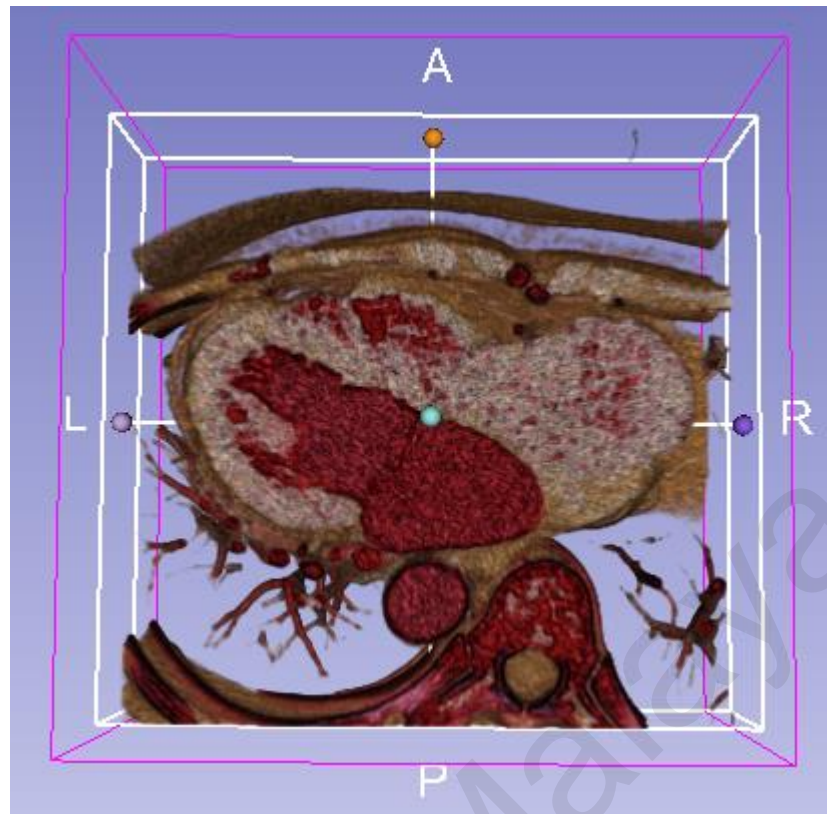
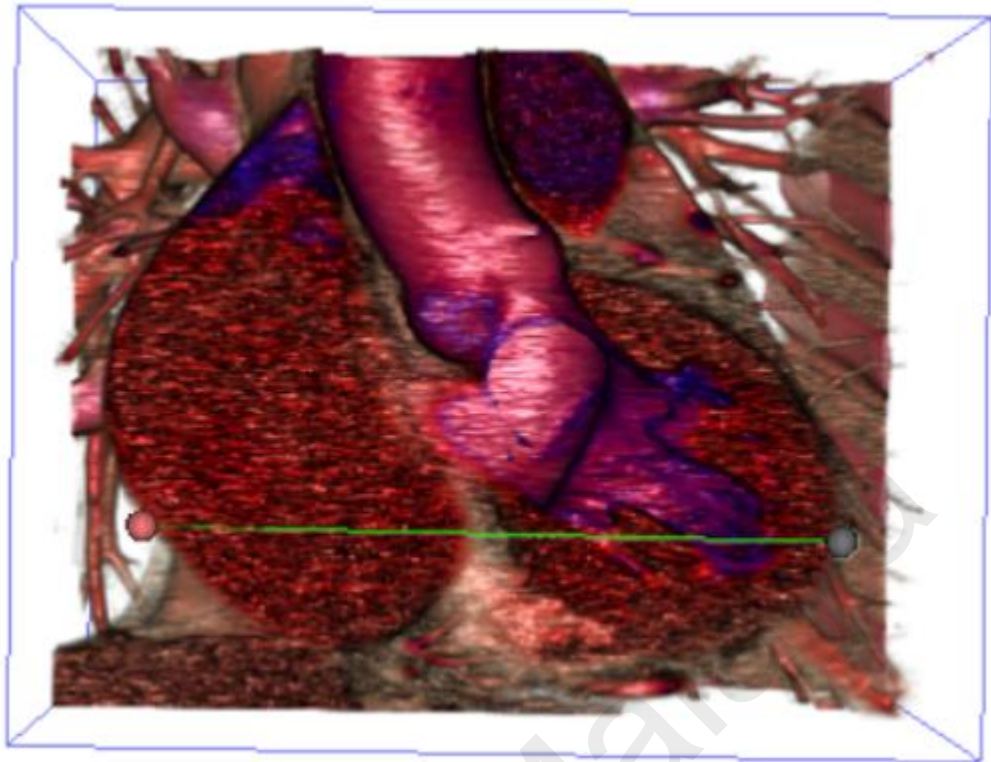


Figure 4. 16: Four Chamber view of the heart using 3D slicer

The Two chamber view and three chamber view of the heart is not possible using 3D slicer as the plane can only be sliced at right angle, thus preventing the 3D model to be sliced diagonally as required for the display of the two-chamber view and three chamber view of the heart.

4.3. Measurement of the heart using VTK and 3D slicer

The distance between two points can be measured using both VTK and 3D slicer. This allows the length, width and height of the heart to be determined. The measurement of the width, height and length of the heart is 125.3 mm, 123.4 mm and 72.4 mm respectively using VTK while the corresponding measurement using 3D slicer are 128.6 mm, 117.4 mm and 76.13 mm respectively



The length of two points is 12.53297 cm

Figure 4. 17: Width of the heart measurement using VTK

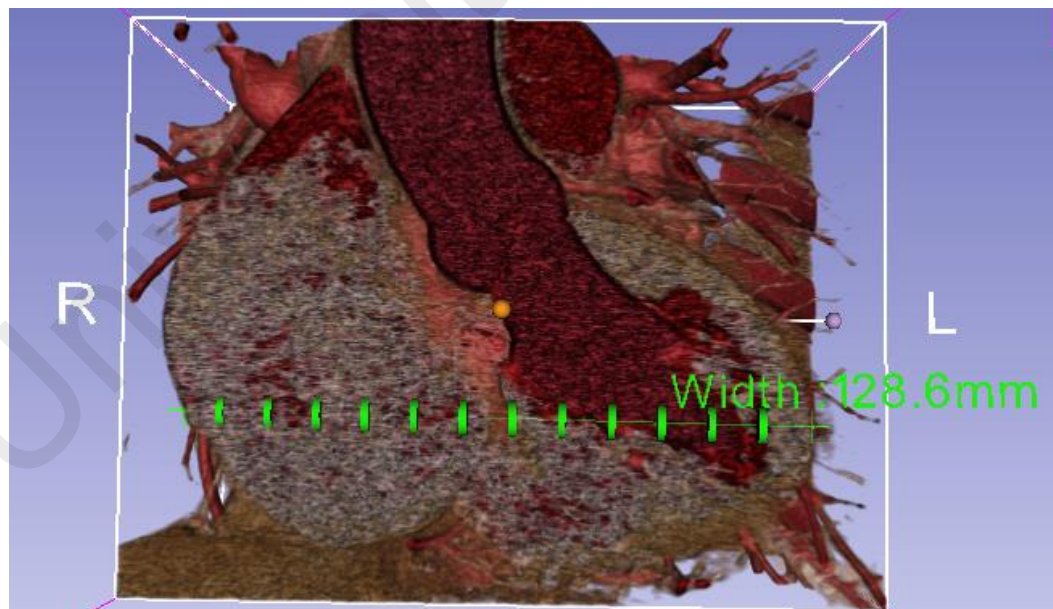
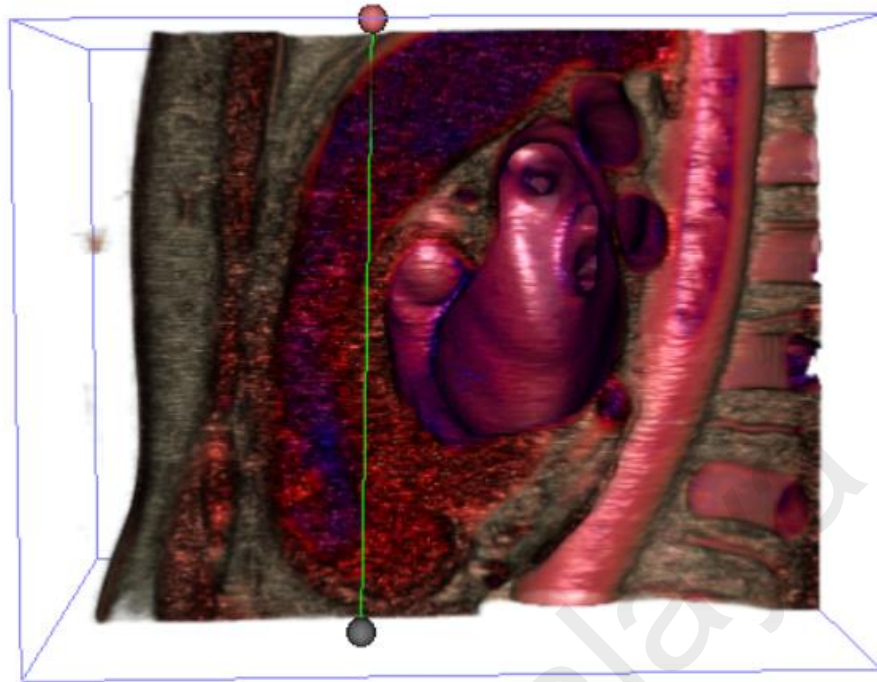


Figure 4. 18: Width of the heart measurement using 3D slicer



The length of two points is 12.34148 cm

Figure 4. 19: Height of the heart measurement using VTK

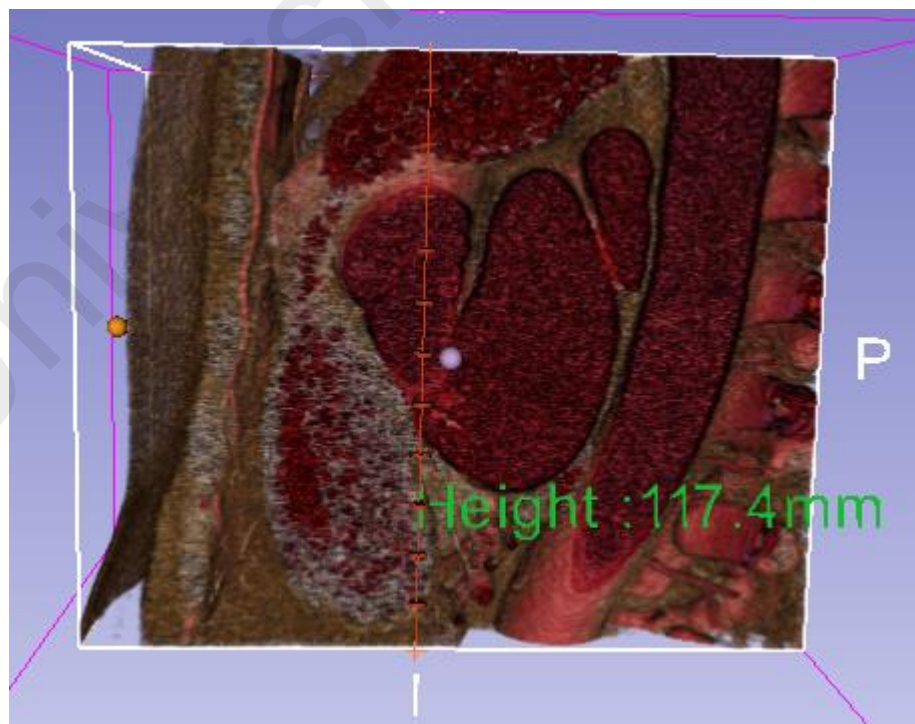
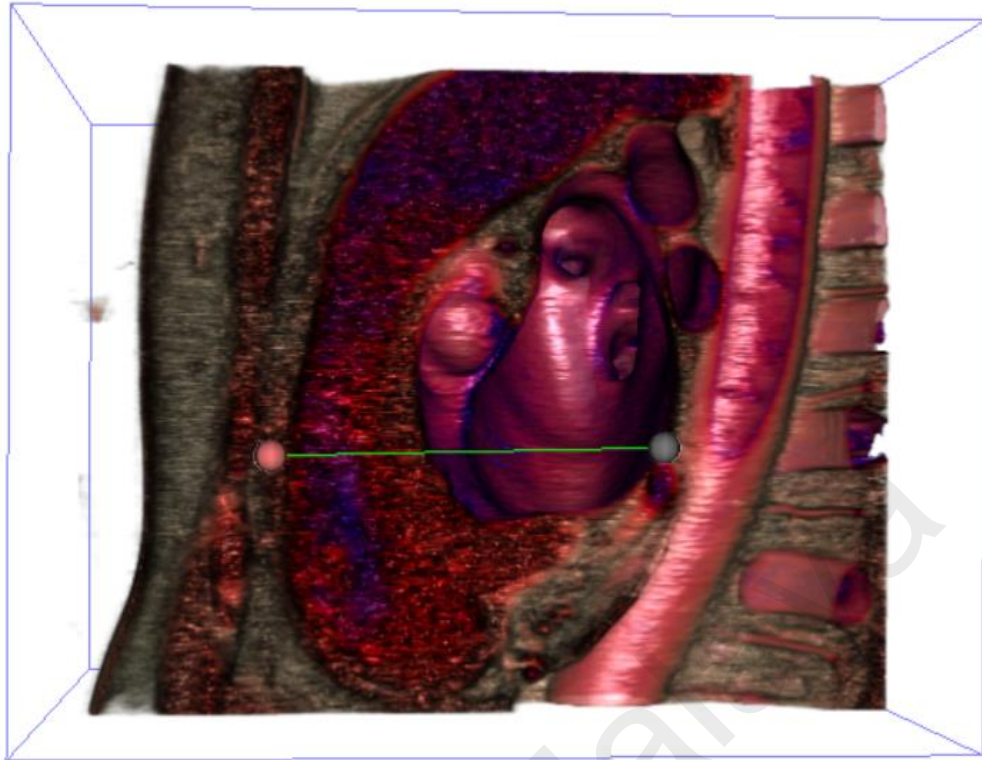


Figure 4. 20: Height of the heart measurement using 3D slicer



The length of two points is 7.24591 cm

Figure 4. 21: Length of the heart measurement using VTK

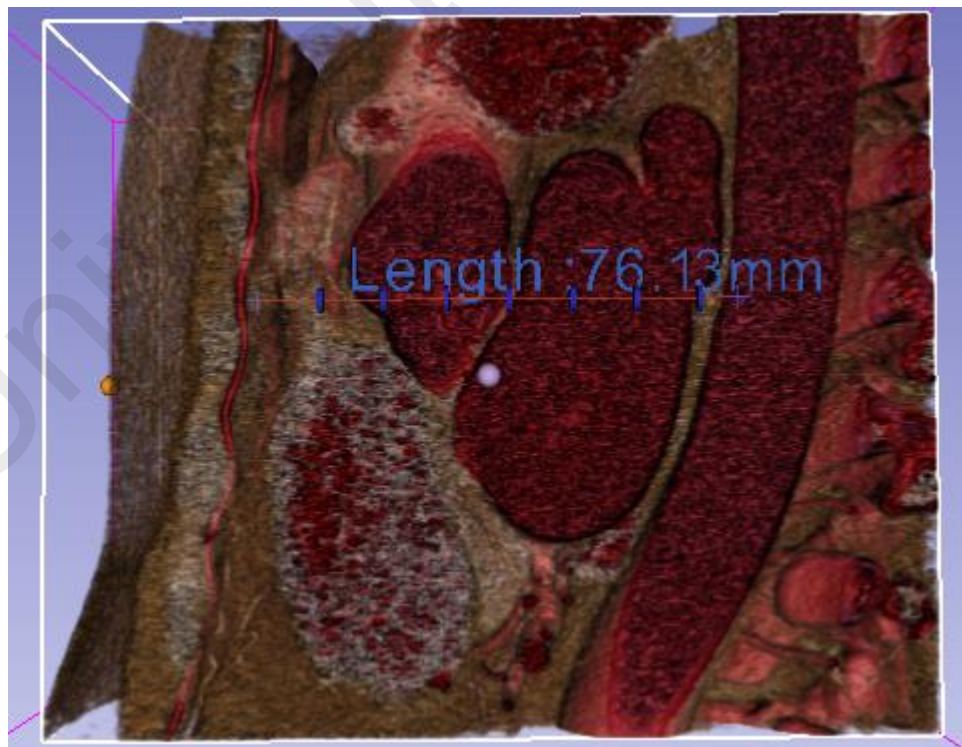


Figure 4. 22: Length of the heart measurement using 3D slicer

CHAPTER 5: DISCUSSIONS

5.1. 3D Reconstruction of Cardiac Chamber Image

The 3D reconstruction of CT images using VTK software allows the cardiac chamber to be visualized more clearly for identification of any anomalies in the form of blockages, tumours and deformities. It also allows the 3D models to be dissected in any angle and viewed from different planes, thus allowing better identification of anomalies not easily identified using 2D images. In this study, a successful 3D model of the heart was constructed from layers of 2D CT scan images. Aside from using the axial, coronal and sagittal view of the heart, VTK also enables the use of two chamber, three chamber and four chamber view of the heart which would allow easier identification of certain anomalies such as ventricular dilation and septal aneurysm. Although none is identified in the model used in this study, should it be present, it is certainly easier to be identified using the 3D model when compared to by just using 2D images. Additionally, less training time is required to identify anomalies inside the heart chamber using the 3D model when compared to the 2D CT scan images which requires expertise knowledge.

The quicker, easier and more accurate identification of malformities would enable quicker action to be taken to treat the disease and medical conditions thus preventing it from deteriorating further which could save lives. Patients are also more likely to be better informed and understand the severity of their medical conditions when it is shown in 3D model as oppose to 2D CT scan images which are quite nebulous and requires a bit more imagination to be visualized in the average person's mind. Therefore, the use of VTK software in reconstructing 3D model for detecting anomalies is highly recommended. Nevertheless, several issues are identified during the 3D reconstruction of cardiac chamber images using VTK.

5.1.1. Visualization of the Right Atrium and the Right Ventricle

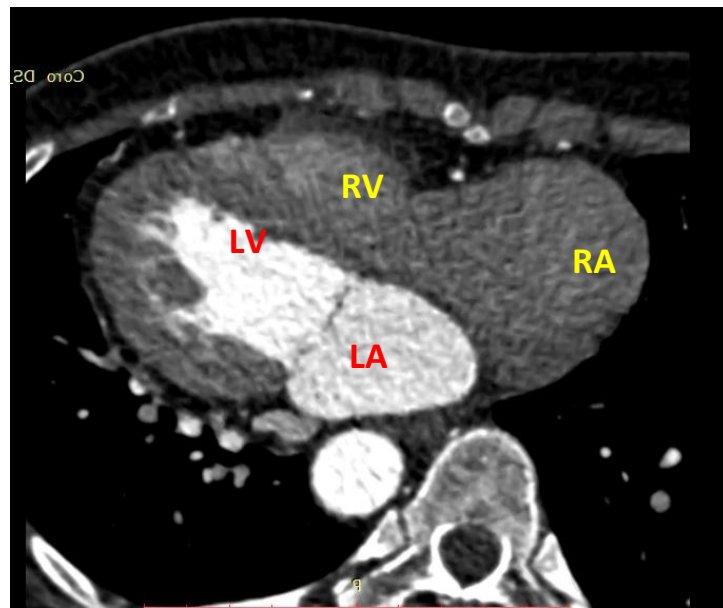


Figure 5. 1: Source image.

As we can see in **Figure 5.1**, which is one of the source images of the CT scans, the right atrium and right ventricle showed very bad contrast. As a result, the right atrium and right ventricle in **Figure 4.4**, **Figure 4.5**, and **Figure 4.8** are barely visible. One possible explanation of this phenomena is that contrast agent was only injected into the left atrium and left ventricle which were the parts of interest of the doctor.

Efforts were made to improve the image at the right ventricle and right atrium. With the opacity and color settings below, a 3D model where the right atrium and right ventricle are visible can be generated. However, some structures in the heart were compromised especially the heart septum. They are shown in **Figure 5.2** (4 Chamber View) and **Figure 5.3** (Sagittal View).

```
vtkPiecewiseFunction *opacityTransferFunction = vtkPiecewiseFunction::New();  
  
//For RA & RV  
opacityTransferFunction->AddPoint(1024*0, 0.00);  
opacityTransferFunction->AddPoint(1024*15, 0.00);  
opacityTransferFunction->AddPoint(1024*20, 1.00);  
opacityTransferFunction->AddPoint(1024*50, 1.00);  
opacityTransferFunction->AddPoint(1024*55, 0.50);  
opacityTransferFunction->AddPoint(1024*60, 0.005);  
opacityTransferFunction->AddPoint(1024*120, 0.001);  
opacityTransferFunction->AddPoint(1024*200, 0.00);
```

```

vtkColorTransferFunction *colorTransferFunction = vtkColorTransferFunction::New();

//For RA & RV
colorTransferFunction->AddRGBPoint(1024+0, 0.0, 0.0, 0.0);
colorTransferFunction->AddRGBPoint(1024+15, 0.0, 0.0, 0.0);
colorTransferFunction->AddRGBPoint(1024+20, 1.0, 0.2, 0.2);
colorTransferFunction->AddRGBPoint(1024+50, 1.0, 0.2, 0.2);
colorTransferFunction->AddRGBPoint(1024+55, 1.0, 0.2, 0.2);
colorTransferFunction->AddRGBPoint(1024+60, 0.0, 0.0, 1.0);
colorTransferFunction->AddRGBPoint(1024+120, 0.0, 0.0, 1.0);
colorTransferFunction->AddRGBPoint(1024+170, 1.0, 1.0, 1.0);

```

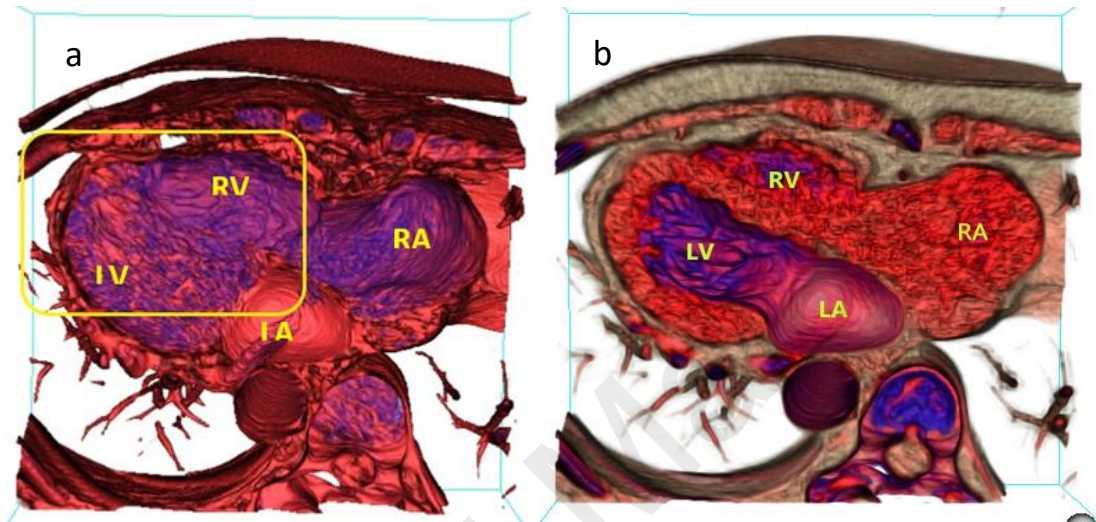


Figure 5. 2: (a) Four Chamber View of the heart where the right atrium and right ventricle are made visible after opacity and colour setting adjustment. The yellow box shows the area where the structure of the septum is compromised. (b) Four Chamber View of the heart in the original setting where the right atrium and right ventricle is barely visible

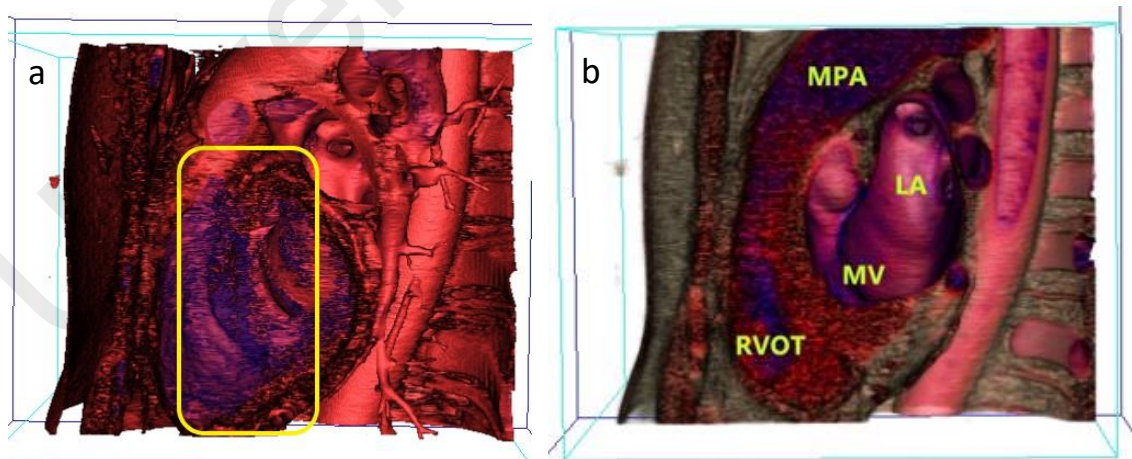


Figure 5. 3: Sagittal View of the heart. (a) The yellow box indicates the area where the structure of the septum is compromised after some adjustment in opacity and colour setting to make the right atrium and ventricle more visible. (b) Sagittal View of the heart in the original setting where the right ventricle is barely visible

5.1.3. Image Noise Reduction

CT scan images usually contained a significant amount of noise which often resulted in grainy and coarse images. The use of photo editing software's filter to reduce the noise is therefore highly recommended. The resultant images as shown in **Figure 5.4** and **Figure 5.5** are clearer, sharper, less grainy and with better contrast.

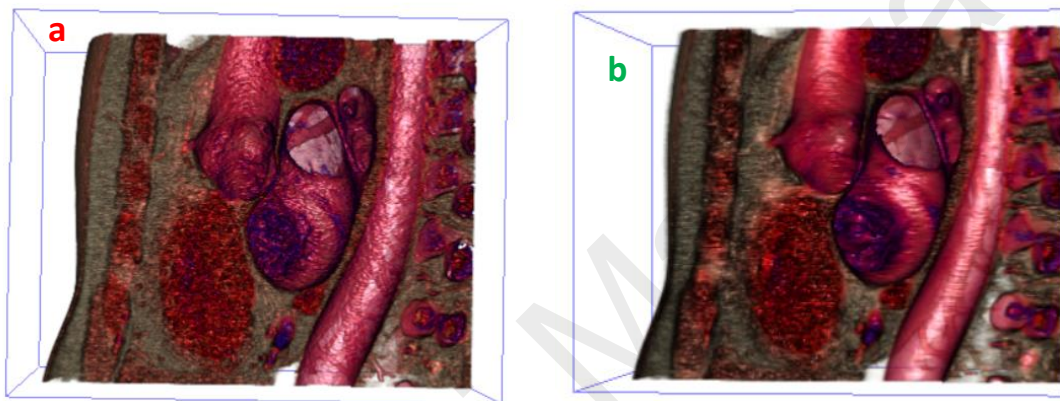


Figure 5. 4: Sagittal view of the heart (a) before and (b) after image noise reduction

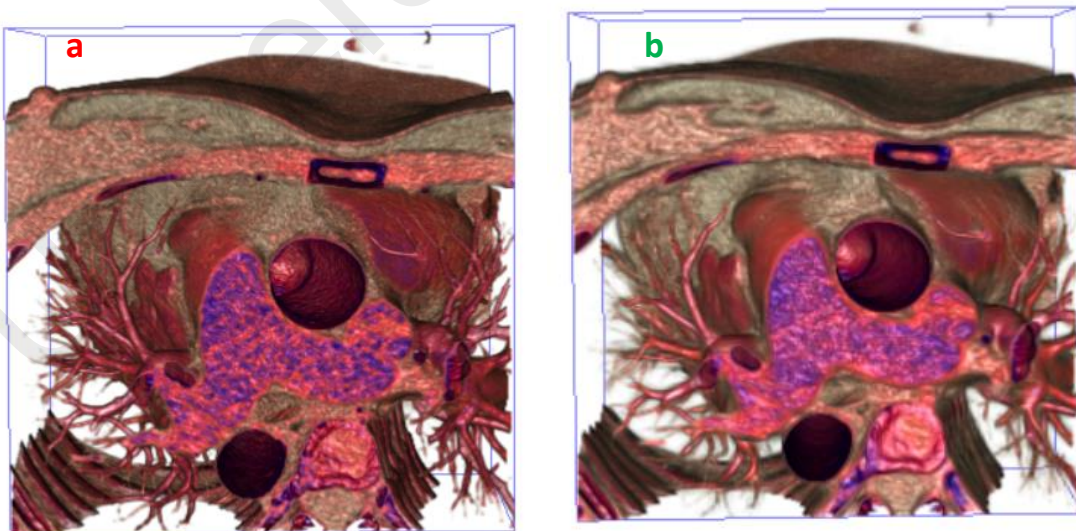


Figure 5. 5: Axial view of the heart (a) before and (b) image noise reduction

5.1.4. Comparison with Surface Rendering Images

By way of comparison, the 3D images generated using the volume rendering method are compared with similar image generated using the surface rendering method (**Figure 5.6, Figure 5.7 & Figure 5.8**). Only the middle layers of the CT scan images are used due to limited processing power.

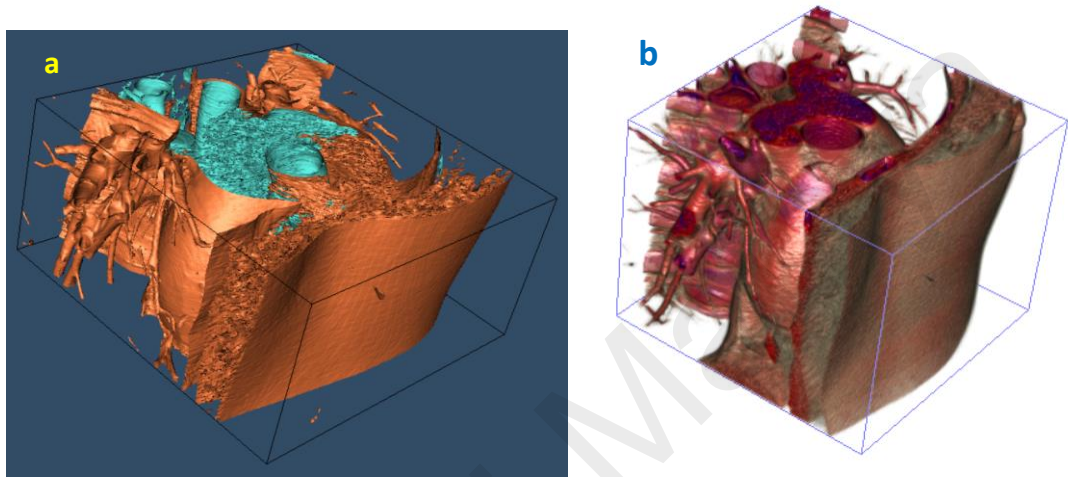


Figure 5. 6: Isometric view of the overall model using the (a) surface rendering technique and (b) volume rendering technique

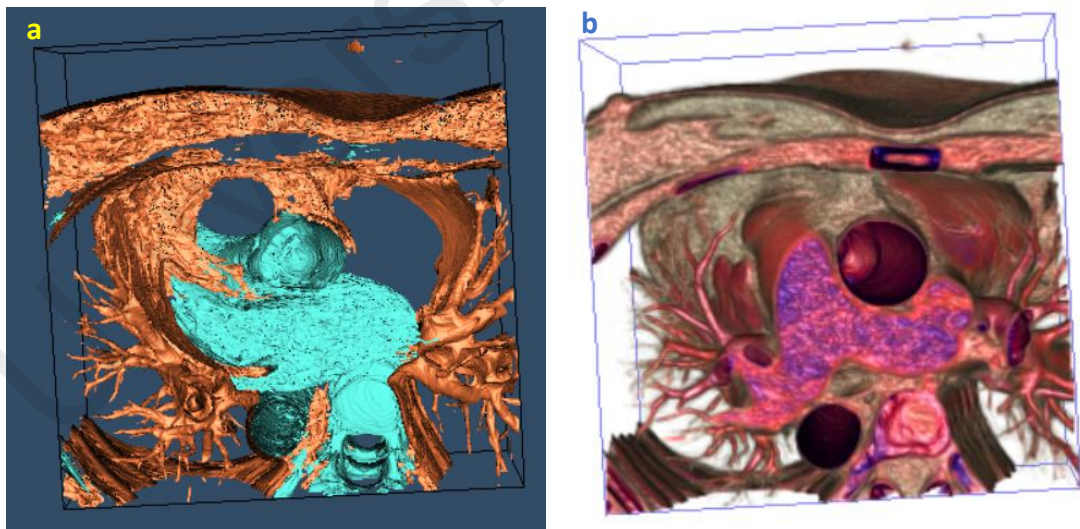


Figure 5. 7: Axial view of the heart using (a) surface rendering method and (b) volume rendering method

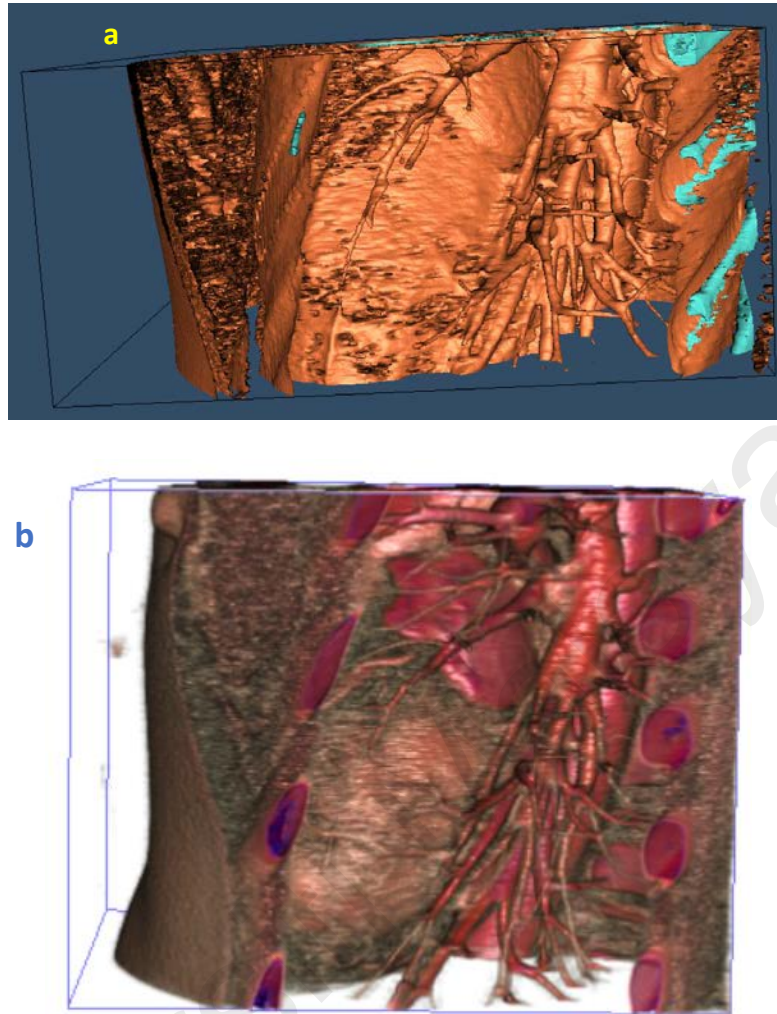


Figure 5. 8: Sagittal view of the heart generated using (a) surface rendering method and (b) volume rendering method

The surface rendering method enables the 3D visualization of the general surface structures of the heart although it has limited usage in investigating and detecting anomalies within the inner chamber of the heart itself. It only generates surface images while the inner structures of the heart remain unknown thus limiting the utility of this method. This suggests volume rendering method as a superior method in visualizing the inner chambers of the heart.

5.2. Comparison with image produced using 3D slicer

Both VTK and 3D slicer software allows 2D CT images to be reconstructed into a 3D model for better visualization. The images produced using VTK is much better and also allows the inner chamber of the heart to be visualized more clearly. Although the 3D model produced using 3D slicer looks good in visualizing the external layers of the heart, the inner chambers of the heart appear flat which prevents the internal contours and condition of the heart chamber to be viewed easily. Therefore, limited information regarding the inner chamber of the heart can be obtained using 3D slicer. Additionally, since the 3D model can only be sliced at right angle, the anomalies that can be identified using 3D slicer are also limited when compared to what can be obtained using VTK as it cannot produced two chamber and three chamber view of the heart which can only be obtained by slicing the 3D model diagonally. Therefore, in terms of visualizing the inner chamber of the heart, VTK is a superior option when compared to 3D slicer.

That being said, it is much easier to generate a 3D model of the heart using 3D slicer as it has pre-set option that specialized in visualizing specific parts of the body thus dispensing the initial need to manually adjust the opacity and colour of the different layers of tissues in the images under investigation. Image of different parts of the body can thus be automatically generated without much adjustment. It is thus much easier for the average user to use when compared to VTK which requires some programming input. 3D slicer also allows the axial, coronal and sagittal views of the heart to be viewed at the same time which helps to pinpoint and identify the object of interest.

In order to substantiate the finding of this research, another 3D model was reconstructed using another data set of 211 cardiac CT scan images from a male patient at RSUP dr Hasan Sadikin (data set 2). The 3D models were generated using the same opacity and colour transfer function setting as well as the general setting. The result shows similar findings whereby the image generated by using VTK software is superior to the

ones produced using 3D slicer especially with regards to visualizing the contours of the inner chambers of the heart.

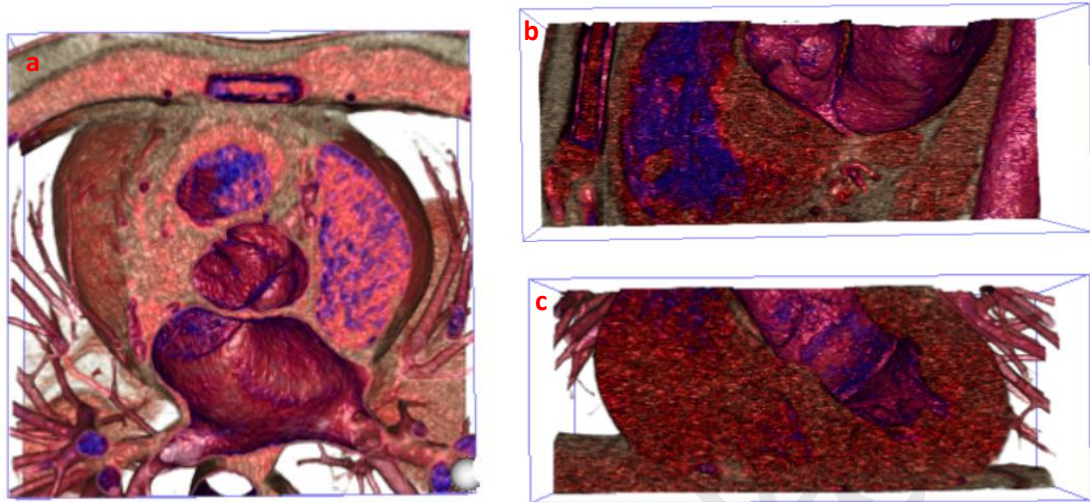


Figure 5. 9: (a) Axial, (b) sagittal and (c) coronal view of the heart generated using data set 2 through VTK programme.

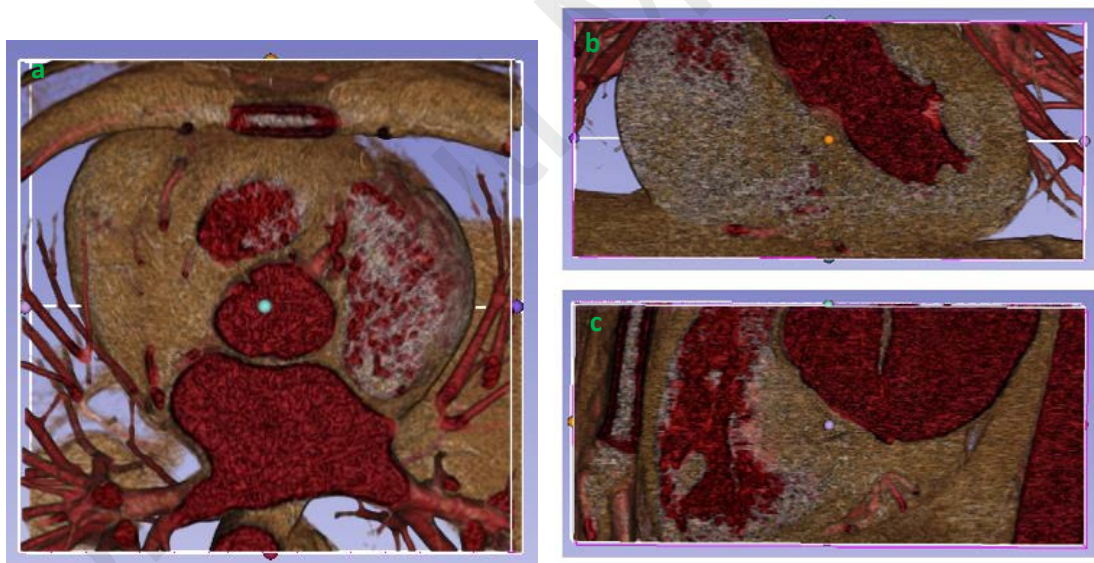


Figure 5. 10: (a) Axial, (b) coronal and (c) sagittal view of the heart generated using data set 2 through 3D slicer programme.

5.3. Measurement of the heart using VTK and 3D slicer

The measurement of the heart using VTK and 3D slicer are slightly different. This is due to the fact that the heart chamber images used in VTK 3D visualization is in JPEG format thus the pixel size is unknown. Adjustment in the codings are needed to assign the correct pixel size for the images used in order to obtain the accurate measurement. This can be determined from DICOM file of the images. On the other hand, the pixel size need not be adjusted using 3D slicer as it had been accurately assigned. That being said, measurement of the heart length, width and height are quite hard to be determined precisely using both software as it is quite hard to select the precise point in 3D space using both software. This may result in two points selected that may not exactly be parallel to the desired image plane. Since the two points selected are angled not parallel to the image plane, the value measured would be varied and imprecise. Therefore, both software are not ideal in measuring the precise length of an object although a rough estimate can be determined.

CHAPTER 6: CONCLUSION

The 3D model of the heart was successfully generated using the VTK programme. No observable clogging was observed in the heart chambers and the arteries of the heart.

3D model reconstructed from layers of 2D CT scan images through the VTK software provides a good opportunity for the visualization of the heart's inner chamber. It is important that a clear 3D image to be reconstructed for a much accurate and easier identification of anomalies and diseases. The quality of the 3D image produced also depends on the source of 2D CT scan images used. More often than not, it contains certain amount of noise which necessitate the use of photo modification software to reduce the noise. This ensures a sharper and clearer image that can provide better contrast for better visualization of the 3D model constructed.

3D reconstruction of the heart chamber using layers of 2D CT image is also possible using the 3D slicer software. Although the resultant 3D model produced gives good quality image of the external surface of the heart, the images does not give good visibility of the inner chamber of the heart as it appears to be grainy and flat. As such, determining anomalies inside the chamber of the heart using 3D slicer is not practical. Therefore, in terms of visualizing the inner chamber of the heart, VTK appears to be the superior option.

Both VTK and 3D slicer has the capability to measure distance between two points. However, the difficulty in pointing or selecting the intended point precisely in 3D spaces hinders the ability of both software in measuring the length of an object precisely. Therefore, the measurement of width, length and height of the heart using both software should only be treated as a rough estimate and not a precise measurement.

Several improvements on the study can be done in future works especially with regards to subject matter expert evaluation. Evaluation of the 3D model generated can be sought from experts in the field like medical imaging specialist, radiologist, cardiologist and

surgeons to further confirm the utility of the 3D model generated. Additionally, the number of software utilized in generating the 3D model should also be increased in future works besides VTK and 3D slicer in other to provide a more comprehensive comparison and evaluation. In the future, the number of CT scan image slices in each data sets used for generating the 3D model should also be increased in order to provide a higher quality 3D model. The number of 3D heart model generated in this study is also limited. It is mainly generated from 1 data set and substantiated with another data set both from RSUP dr Hasan Sadikin hospital. In order to provide a more comprehensive result, at least 3 data set should be utilized for 3D model reconstruction in future works.

Overall, VTK is a good software to be used in visualizing the inner chamber of the heart to detect anomalies by reconstructing 3D model from layers of 2D images.

REFERENCES

- Aboudara, C., Hatcher, D., Nielsen, I., & Miller, A. (2003). A three-dimensional evaluation of the upper airway in adolescents. *Orthodontics and Craniofacial Research*, 6(s1), 173–175. doi:10.1034/j.1600-0544.2003.253.x
- Bell, J.T. (2004). Visualization Tool Kit (VTK) Tutorial. <https://www.cs.uic.edu/~jbell/CS526/Tutorial/Tutorial.html>
- Caban, J. J., Joshi, A., & Nagy, P. (2007). Rapid Development of Medical Imaging Tools with Open-Source Libraries. *Journal of Digital Imaging*, 20(S1), 83–93. doi:10.1007/s10278-007-9062-3
- Calhoun, P. S., Kuszyk, B. S., Heath, D. G., Carley, J. C., & Fishman, E. K. (1999). Three-dimensional Volume Rendering of Spiral CT Data: Theory and Method. *RadioGraphics*, 19(3), 745–764. doi:10.1148/radiographics.19.3.g99ma14745
- Chang, J., Zhang, X., Zhang, K., & Pan, Q. (2019). Three-dimensional reconstruction of medical images based on 3D slicer. *Journal of Complexity in Health Sciences*, 2(1), 1–12. doi:10.21595/chs.2019.20724
- Chaosuwannakit N. (2018). Anatomical variants and coronary anomalies detected by dual-source coronary computed tomography angiography in North-eastern Thailand. *Polish journal of radiology*, 83, e372–e378. <https://doi.org/10.5114/pjr.2018.78420>
- Choi, J. H., Baek, S. Y., Kim, Y., Son, T. G., Park, S., & Lee, K. (2014). Automatic detection of inferior alveolar nerve canal from cone-beam computed tomography images for dental surgery planning. *Studies in health technology and informatics*, 196, 61–65.
- Dalrymple, N. C., Prasad, S. R., Freckleton, M. W., & Chintapalli, K. N. (2005). Introduction to the Language of Three-dimensional Imaging with Multidetector CT. *RadioGraphics*, 25(5), 1409–1428. doi:10.1148/rg.255055044
- Dong, H., Xia, L., Peng, Z., & Zhang, J. (2012). 3D-Visualization for DICOM Series Based on ITK and VTK. *Applied Mechanics and Materials*, 263–266, 2530–2533. <https://doi.org/10.4028/www.scientific.net/amm.263-266.2530>
- Fedorov, A., Beichel, R., Kalpathy-Cramer, J., Finet, J., Fillion-Robin, J. C., Pujol, S., Bauer, C., Jennings, D., Fennessy, F., Sonka, M., Buatti, J., Aylward, S., Miller,

- J. V., Pieper, S., & Kikinis, R. (2012). 3D Slicer as an image computing platform for the Quantitative Imaging Network. *Magnetic resonance imaging*, 30(9), 1323–1341. <https://doi.org/10.1016/j.mri.2012.05.001>
- Fishman, E. K., Magid, D., Ney, D. R., Chaney, E. L., Pizer, S. M., Rosenman, J. G., ... Robertson, D. D. (1991). *Three-dimensional imaging*. *Radiology*, 181(2), 321–337. doi:10.1148/radiology.181.2.1789832
- Frericks, B. B., Caldarone, F. C., Nashan, B., Savellano, D. H., Stamm, G., Kirchhoff, T. D., ... Galanski, M. (2004). 3D CT modeling of hepatic vessel architecture and volume calculation in living donated liver transplantation. *European Radiology*, 14(2), 326–333. doi:10.1007/s00330-003-2161-8
- Ghoshal, S., Banu, S., Chakrabarti, A., Sur-Kolay, S. and Pandit, A. (2020), 3D reconstruction of spine image from 2D MRI slices along one axis. *IET Image Process.*, 14: 2746-2755. <https://doi.org/10.1049/iet-ipr.2019.0800>
- Ginat, D. T., Fong, M. W., Tuttle, D. J., Hobbs, S. K., & Vyas, R. C. (2011). Cardiac imaging: Part 1, MR pulse sequences, imaging planes, and basic anatomy. *AJR. American journal of roentgenology*, 197(4), 808–815. <https://doi.org/10.2214/AJR.10.7231>
- Goo, H. W., Park, I.-S., Ko, J. K., Kim, Y. H., Seo, D.-M., & Park, J.-J. (2005). Computed tomography for the diagnosis of congenital heart disease in pediatric and adult patients. *The International Journal of Cardiovascular Imaging*, 21(2-3), 347–365. doi:10.1007/s10554-004-4015-0
- Hafizah, M., Kok, T., & Supriyanto, E. (2010). Development of 3D image reconstruction based on untracked 2D fetal phantom ultrasound images using VTK. *WSEAS Transactions on Signal Processing archive*, 6, 145-154.
- Karatas, O., & Toy, E. (2014). Three-dimensional imaging techniques: A literature review. *European Journal of Dentistry*, 8(1), 132. doi:10.4103/1305-7456.126269
- Kim, J., Jung, Y., Feng, D. D., & Fulham, M. J. (2020). Biomedical image visualization and display technologies. *Biomedical Information Technology*, 561–583. doi:10.1016/b978-0-12-816034-3.00017-1
- Koo, H. J., Yang, D. H., Kang, J. W., Lee, J. Y., Kim, D. H., Song, J. M., Kang, D. H., Song, J. K., Kim, J. B., Jung, S. H., Choo, S. J., Chung, C. H., Lee, J. W., & Lim, T. H. (2018). Demonstration of infective endocarditis by cardiac CT and transoesophageal echocardiography: comparison with intra-operative

- findings. *European heart journal. Cardiovascular Imaging*, 19(2), 199–207. <https://doi.org/10.1093/ehjci/jex010>
- Krans, B. (2017). Heart CT Scan. *Healthline*. <https://www.healthline.com/health/heart-ct-scan>
- Krupinski E. A. (2010). Current perspectives in medical image perception. *Attention, perception & psychophysics*, 72(5), 1205–1217. <https://doi.org/10.3758/APP.72.5.1205>
- Lichtenbelt, B.B., Crane, R., & Naqvi, S. (1998). Introduction to volume rendering.
- Masutani, Y., MacMahon, H., & Doi, K. (2001). Automated Segmentation and Visualization of the Pulmonary Vascular Tree in Spiral CT Angiography: An Anatomy-Oriented Approach Based on Three-Dimensional Image Analysis. *Journal of Computer Assisted Tomography*, 25(4), 587–597. doi:10.1097/00004728-200107000-00014
- Mamdouh, R., El-Bakry, H., Riad, A., & El-Khamisy, N. (2020). Converting 2D-Medical Image Files “DICOM” into 3D- Models, Based on Image Processing, and Analysing Their Results with Python Programming. *WSEAS Transactions on Computers*. 19. 10-20. 10.37394/23205.2020.19.2.
- Ou, P., Celermajer, D. S., Calcagni, G., Brunelle, F., Bonnet, D., & Sidi, D. (2007). Three-dimensional CT scanning: a new diagnostic modality in congenital heart disease. *Heart (British Cardiac Society)*, 93(8), 908–913. <https://doi.org/10.1136/hrt.2006.101352>
- O’Brien, J. P., Srichai, M. B., Hecht, E. M., Kim, D. C., & Jacobs, J. E. (2007). Anatomy of the Heart at Multidetector CT: What the Radiologist Needs to Know. *RadioGraphics*, 27(6), 1569–1582. doi:10.1148/rg.276065747
- Ou, P., Celermajer, D. S., Calcagni, G., Brunelle, F., Bonnet, D., & Sidi, D. (2007). Three-dimensional CT scanning: a new diagnostic modality in congenital heart disease. *Heart*, 93(8), 908–913. doi:10.1136/hrt.2006.101352
- Paik, D.S., Beaulieu, C.F., Jeffrey, R.B., Rubin, G.D. and Napel, S. (1998), Automated flight path planning for virtual endoscopy. *Med. Phys.*, 25: 629-637. <https://doi.org/10.1118/1.598244>
- Pan, Y.-N., Li, A.-J., Chen, X.-M., Wang, J., Ren, D.-W., & Huang, Q.-L. (2016). Coronary Computed Tomographic Angiography at Low Concentration of

Contrast Agent and Low Tube Voltage in Patients with Obesity. *Academic Radiology*, 23(4), 438–445. doi:10.1016/j.acra.2015.12.007

Pei, G. (2019). Digital Orthopedics. doi:10.1007/978-94-024-1076-1

Sato, Y., Shiraga, N., Nakajima, S., Tamura, S., & Kikinis, R. (1998). Local maximum intensity projection (LMIP): a new rendering method for vascular visualization. *Journal of computer assisted tomography*, 22(6), 912–917. <https://doi.org/10.1097/00004728-199811000-00014>

Schroeder, S., Achenbach, S., Bengel, F., Burgstahler, C., Cademartiri, F., de Feyter, P., ... Bax, J. J. (2008). Cardiac computed tomography: indications, applications, limitations, and training requirements: Report of a Writing Group deployed by the Working Group Nuclear Cardiology and Cardiac CT of the European Society of Cardiology and the European Council of Nuclear Cardiology. *European Heart Journal*, 29(4), 531–556. doi:10.1093/eurheartj/ehm544

Semba, C. P., Rubin, G. D., & Dake, M. D. (1994). Three-dimensional spiral CT angiography of the abdomen. *Seminars in Ultrasound, CT and MRI*, 15(2), 133–138. doi:10.1016/s0887-2171(05)80095-2

Summers, R. M., Beaulieu, C. F., Pusanik, L. M., Malley, J. D., Jeffrey, R. B., Glazer, D. I., & Napel, S. (2000). Automated Polyp Detector for CT Colonography: Feasibility Study. *Radiology*, 216(1), 284–290. doi:10.1148/radiology.216.1.r00jl43284

Taylor, A. M., Dymarkowski, S., Hamaekers, P., Razavi, R., Gewillig, M., Mertens, L., & Bogaert, J. (2005). MR Coronary Angiography and Late-Enhancement Myocardial MR in Children Who Underwent Arterial Switch Surgery for Transposition of Great Arteries. *Radiology*, 234(2), 542–547. doi:10.1148/radiol.2342032059

Tubiana M. (1996). Wilhelm Conrad Röntgen et la découverte des rayons X [Wilhelm Conrad Röntgen and the discovery of X-rays]. *Bulletin de l'Academie nationale de medecine*, 180(1), 97–108.

Udupa, J. K. (1999). Three-dimensional Visualization and Analysis Methodologies: A Current Perspective. *RadioGraphics*, 19(3), 783–806. doi:10.1148/radiographics.19.3.g99ma13783

Wang D., Ma D., Wong M.L., Wáng Y.X. (2015). Recent advances in surgical planning & navigation for tumor biopsy and resection. *Quantitative Imaging in Medicine & Surgery*, 5(5):640-648. doi: 10.3978/j.issn.2223-4292.2015.10.03

- Wang, H., & Pu, X. (2009). 3D Medical CT Images Reconstruction Based on VTK and Visual C++. *2009 3rd International Conference on Bioinformatics and Biomedical Engineering*. doi:10.1109/icbbe.2009.5162140
- Willems, T., & Hazewinkel, M. (February 13, 2009). Cardiac Anatomy. *Radiology Assistant*. <https://radiologyassistant.nl/cardiovascular/anatomy/cardiac-anatomy>
- World Health Organization. (December 9, 2020). The top 10 causes of death. Retrieved from <https://www.who.int/news-room/fact-sheets/detail/the-top-10-causes-of-death>
- Xiong, G., Sun, P., Zhou, H., Ha, S., Hartaigh, B. o, Truong, Q. A., & Min, J. K. (2017). Comprehensive Modeling and Visualization of Cardiac Anatomy and Physiology from CT Imaging and Computer Simulations. *IEEE Transactions on Visualization and Computer Graphics*, 23(2), 1014–1028. doi:10.1109/tvcg.2016.2520946
- Yan, R. G., Guo, X. D., & Xu, C. (2012). Reconstruction and visualization of human gastrointestinal tract. *International journal of biomedical science : IJBS*, 8(1), 22–27.
- Yin, D., & Lu, R. (2015). A Method of Breast Tumour MRI Segmentation and 3D Reconstruction. *2015 7th International Conference on Information Technology in Medicine and Education (ITME)*, 23-26.
- Zezo. (October 27, 2020). Step-by-Step Analysis of Cardiac Chambers in CT. *Radiology Key*. Retrieved from <https://radiologykey.com/step-by-step-analysis-of-cardiac-chambers-in-ct/>
- Zhi, X., Zhang, Z., Gao, Y., & Zhang, Z. (2013). Real-Time Vascular Beating Analog Based on the Mass-Spring Model. *2013 Ninth International Conference on Intelligent Information Hiding and Multimedia Signal Processing*. doi:10.1109/iih-msp.2013.55